

Capacity Characterization for Reconfigurable Intelligent Surfaces Assisted Multiple-Antenna Multicast

Linsong Du^{ID}, *Student Member, IEEE*, Shihai Shao^{ID}, *Member, IEEE*, Gang Yang^{ID}, *Member, IEEE*, Jianhui Ma, *Member, IEEE*, Qingpeng Liang^{ID}, *Member, IEEE*, and Youxi Tang, *Member, IEEE*

Abstract—The reconfigurable intelligent surface (RIS), which consists of a large number of passive and low-cost reflecting elements, has been recognized as a revolutionary technology to enhance the performance of future wireless networks. This paper considers an RIS assisted multicast transmission, where a base station (BS) with multiple-antenna multicasts common message to multiple single-antenna mobile users (MUs) under the assistance of an RIS. An equivalent channel model for the considered multicast transmission is analyzed, and then an optimization problem for the corresponding channel capacity is formulated to obtain the optimal covariance matrix and phase shifts. In order to solve the above non-convex and non-differentiable problem, this paper first exploits the gradient descent method and alternating optimization, to approach the locally optimal solution for any number of MUs. Then, this paper considers a special case, which can obtain the global optimal solution, and shows the sufficient and necessary condition for this special case. Finally, the order growth of the maximal capacity is obtained when the numbers of the reflecting elements, the BS antennas, and the MUs go to infinity.

Index Terms—Reconfigurable intelligent surfaces, capacity characterization, multicast transmission.

I. INTRODUCTION

IN future cellular networks, with the increased demands of sending common messages to multiple mobile users (MUs), such as music sharing, video streaming, and pictures downloading [1], the application of multiple antenna multicast

transmission becomes more promising for sending common messages to multiple MUs with the high transmission rate [2]. When compared with the unicast transmission, where the base station (BS) only servers one MU during one time slot, multicast transmission can significantly reduce energy consumption and save spectral resources [2]. However, in many multicast scenarios [3], the direct link from the BS to MUs is blocked, due to the existence of buildings, trees, and cars. In order to overcome this problem, an effective solution is to add a new link to maintain multicast communication. Moreover, the capacity of the multicast communication only depends on the minimum received signal-to-noise ratio among all the BS-MU links. It follows that if any one of the links suffers from bad channel conditions, the multicast capacity will become very low. Therefore, it is best to obtain an effective way to improve the BS-MU links with bad channel conditions.

Therefore, the reconfigurable intelligent surface (RIS) technology is considered to be a new way in the multicast communication, which provide wireless connectivity in future 6G system [4]. The RIS consists of a large number of reconfigurable reflecting elements, each of which can induce the phase shifts of the electromagnetic waves and then reflects them [5]–[8]. The RIS can proactively control the multicast channel between the BS and MUs via highly controllable and intelligent signal reflection. Thus, the RIS provides a new degree of freedom to improve the performance of the multicast communication. It is worth noting that the RIS can be regarded as a no-power full-duplex (FD) amplify-and-forward (AF) relay with multiple-antenna, which receives signals and then forwards them to the MUs. However, there exists some differences between the relay and the RIS as follows. Similar to backscatter [9]–[11], since the RIS does not use the transmit radio frequency (RF) chain, it hardly consumes any energy. Thus, RIS can achieve much higher energy efficiency and is more environmentally-friendly than the regular FD AF relay, and does not cause self-interference as well. In fact, the RIS can achieve a higher rate than the AF relay when the total transmit power (i.e., the sum of the transmit power at the BS and the AF relay) is fixed [12]. Moreover, comparing with massive multiple-input multiple-output (MIMO), the RISs have a less complex structure and lower cost. They are easy to densely deploy at various types of places such as trees, buildings, and rooms [13]. The RIS is able to cater to the different application scenarios. First, the RIS

Manuscript received July 21, 2020; revised November 3, 2020, February 8, 2021, April 20, 2021, and April 29, 2021; accepted April 29, 2021. Date of publication May 18, 2021; date of current version October 11, 2021. This work was supported in part by the National Key Research and Development Program of China under Grant 2018YFB1801903; in part by the National Natural Science Foundation of China under Grant 62071093, Grant 61901396, Grant 62071094, Grant U19B2014, Grant 61771107, Grant 61701075, Grant 61601064, and Grant 61531009; and in part by the Sichuan Science and Technology Program under Grant 2020YFH0101. The associate editor coordinating the review of this article and approving it for publication was H. Pishro-Nik. (*Corresponding authors: Shihai Shao; Gang Yang.*)

Linsong Du, Shihai Shao, Gang Yang, Jianhui Ma, and Youxi Tang are with the National Key Laboratory of Science and Technology on Communications, University of Electronic Science and Technology of China, Chengdu 611731, China (e-mail: linsongdu@outlook.com; ssh@uestc.edu.cn; yanggang@uestc.edu.cn; jianhui.ma@std.uestc.edu.cn; tangyx@uestc.edu.cn).

Qingpeng Liang is with the School of Information Science and Technology, Southwest Jiaotong University, Chengdu 611756, China (e-mail: qingpengliang@gmail.com).

Color versions of one or more figures in this article are available at <https://doi.org/10.1109/TWC.2021.3078853>.

Digital Object Identifier 10.1109/TWC.2021.3078853

can provide a new link to maintain transmission in the dead zone [14]–[17], where the direct paths between the BS and the MUs are blocked by obstacles. Then, the RIS can improve the physical layer security by enhancing the desired signals and suppressing the undesired signals [18]–[21]. In addition, when MU suffers co-channel interference from other interferers, the RIS can be placed to suppress the interference. Finally, indoor environments can be coated with the RIS to increase the throughput offered by conventional access points. Due to the above benefits, the RIS can adaptively adjust the phase shifts of the received signals, it can enhance the BS-MU links with bad channel conditions under indoor and outdoor scenarios. Therefore, this paper focuses on RIS assisted multicast communication.

However, the application of the RIS on multicast communication is confronted with a challenge. In order to optimize the phase shifts at the RIS, the RIS assisted multicast system requires the accurate channel state information (CSI) on the RIS-related channel with the BS and the MUs. The acquisition of CSI on the RIS-related channel is difficult since RIS without any RF chains cannot perform baseband processing functionality. Therefore, the CSI of BS-RIS and RIS-MUs links cannot be separately estimated via the traditional training-based approaches in general [22], [23]. Considering this issue, the authors in [24] considered deploying the dedicated RF chains at RIS to acquire the CSI of RIS-MUs links. However, this approach increases the implementation cost and decreases energy efficiency, which loses the essential benefits of the RIS. Thus, the authors in [25]–[29] proposed the channel estimation methods in multiple MUs scenario to obtain the cascaded CSI of BS-RIS-MU links without using RF chains at the RIS. In [25], [26], the BS can obtain the global CSI of all BS-RIS-MU links by uplink channel estimation due to channel reciprocity, where each MU transmits its pilot symbols to the BS on the different time slots, such that each cascaded CSI of BS-RIS-MU link is estimated by BS. A three-phase channel estimation framework was proposed in [26] to shorten the estimated time. In [27], a transmission protocol was proposed to estimate cascaded CSI of BS-RIS-MU for orthogonal frequency division multiplexing (OFDM) system under unit-modulus constraint. In [28], a fast channel estimation scheme with reduced OFDM symbol duration was proposed for the fading channel. In [29], the SeUCE scheme was proposed to estimate cascaded CSI for multi-user OFDM access system. The cascaded CSI of the BS-RIS-MU link is sufficient for the design of the phase shifts at the RIS and the covariance matrix at the BS.

Based on the available cascaded CSI, the authors [8], [30], [31] studied how to optimize the phase shifts at the RIS in a multicast system. The authors in [30] considered the fair quality of service for multicasting assisted by the RIS and proposed efficient algorithms to optimize the quality of service by jointly designing the transmit beamforming and the phase shifts. The authors in [31] considered the RIS assisted multi-group multicasting and maximized the sum rate of all the multicasting groups by optimizing the transmit beamforming and the phase shifts. However, the works in [30], [31] only study the transmit beamforming vector at BS,

which cannot embody the theoretically maximal achievable rate, i.e., capacity, for RIS assisted multicast communication. The study of capacity indicates the optimal performance achievable on the RIS assisted multicast channel and how to achieve such optimal performance. In order to obtain the capacity, the covariance matrix at BS should be optimized, which brings a new challenge. Indeed, the authors in [24] studied the capacity characterization for the RIS assisted MIMO communications in the unicast scenario. However, the results in [24] cannot generalize to the multicast scenario. The capacity maximization problem in the multicast scenario is more difficult to solve as compared to that in the unicast scenario since the capacity maximization problem in RIS assisted multicast communication is a non-differentiable max-min problem, and phase shifts and covariance matrix need to be designed to balance the different BS-RIS-MU links. To the best of our knowledge, there is no work considering capacity characterization for the RIS assisted multicast communication.

In this paper, we consider the RIS assisted multi-antenna multicast transmission, where a multi-antenna BS sends common messages to a group of single-antenna MUs. An RIS consisting of a large number of reconfigurable reflecting elements is deployed to assist the multicast transmission, where the BS sends signals to the RIS, and then the RIS forwards the received signals to the MUs with phase shifts. It is assumed that the cascaded CSI of BS-RIS-MU links and the CSI of BS-MUs links are perfectly known to the BS and the RIS. The equivalent channel model for the considered multicast system is obtained, which can be regarded as a conventional multicast channel, and its characteristics can be partly controlled by the reconfigurable reflecting elements. Thus, it is crucial to find the optimal phase shifts of the RIS to maximize the capacity of the equivalent channel model. The main contributions of this paper are summarized as follows.

- First, an optimization problem of the channel capacity is formulated to obtain the optimal phase shifts for the RIS and the corresponding covariance matrix of the transmitted symbol vector for the BS. Since this problem is non-convex and non-differentiable, it is difficult to obtain the optimal solution directly. Thus, the non-differentiable problem is reformulated into a differentiable problem. Then, the gradient descent method and alternating optimization, respectively, are proposed to approach a locally optimal solution. We consider a specific case, which owns optimal semi-closed form solution, and show the sufficient and necessary conditions that the special case happens.
- Next, we analyze the order growth of the optimal capacity of RIS assisted multicast transmission in some asymptotic cases: 1) The number of MUs is fixed and the number of antennas or reflecting elements goes to infinity; 2) The numbers of antennas and reflecting elements are fixed, and the number of MUs goes to infinity; 3) The numbers of antennas, reflecting elements, and MUs all go to infinity.
- Finally, we numerically evaluate the performance of the proposed two algorithms, which confirm the asymptotic analysis of optimal capacity. From the numerical results

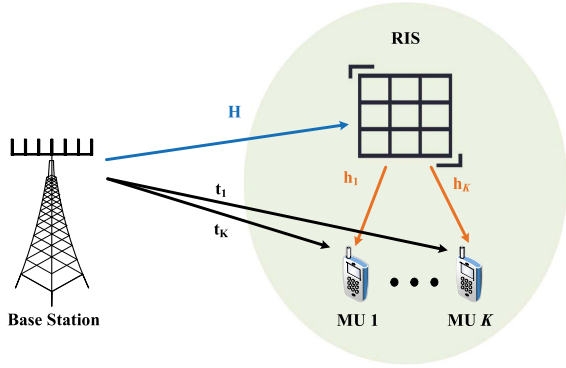


Fig. 1. RIS assisted multicast transmissions with K MUs.

and asymptotic analysis, we observe that the optimal capacity grows logarithmically with the number of antennas and the square of the number of reflecting elements, and it is the inverse proportion with the number of MUs. When both numbers of MUs and antennas go to infinity at a fixed ratio, the optimal capacity remains a constant.

The structure of this paper is organized as follows. Section II introduces the system model and formulates an optimization problem of the channel capacity. Section III proposes two algorithms for optimization problem for any number of MUs. Section IV shows the asymptotic analysis for the capacity of the RIS assisted multicast transmission. Section V presents some numerical results. Section VI concludes the paper.

Notation: \mathbf{a} is a vector, \mathbf{A} is a matrix. $\|\mathbf{a}\|$ is Euclidean norm of \mathbf{a} . \mathbf{A}^H , \mathbf{A}^T , $\|\mathbf{A}\|_{m_2}$, \mathbf{A}^{-1} denote Hermitian transpose, transpose, Frobenius norm and pseudo-inverse of \mathbf{A} , respectively. $\text{diag}(\mathbf{a})$ is a diagonal matrix with the entries of \mathbf{a} on its main diagonal. $\mathbf{A} \succeq \mathbf{B}$ means that $\mathbf{A} - \mathbf{B}$ is positive semidefinite. $\mathbf{A} \otimes \mathbf{B}$ denotes the kronecker product between \mathbf{A} and \mathbf{B} . $\text{Tr}(\mathbf{A})$ denotes the trace of \mathbf{A} . $\mathbb{E}\{\mathbf{A}\}$ denotes the expected value of each element for \mathbf{A} . $\det \mathbf{A}$ denotes the determinant of \mathbf{A} . $\text{vec}(\mathbf{A})$ is an operator that transforms \mathbf{A} into a column vector by vertically stacking the columns of the matrix. $\frac{\mathbf{A}}{x}$ means that the each element of \mathbf{A} divides by x . $\mathbb{C}^{N \times M}$ denotes the set of all $N \times M$ complex-valued matrices. \mathbf{I} is an identity matrix. $j \triangleq \sqrt{-1}$ is the imaginary unit. $\arg(\cdot)$ denotes the argument of a complex number. $\text{Cov}(\cdot, \cdot)$ is covariance.

II. SYSTEM MODEL AND PROBLEM FORMULATION

A. System Model

As shown in Fig. 1, a BS with M -antennas sends a common message to K single-antenna MUs¹ [32], [33]. An RIS with N reflecting elements is deployed between the BS and the K MUs, where the cascaded CSI of BS-RIS-MU link and the CSI of BS-MU link are perfectly known. Accordingly, the received signal at MU k , $k = 1, 2, \dots, K$ is given by

$$y_k = (\mathbf{h}_k^H \Phi \mathbf{H} + \mathbf{t}_k^H) \mathbf{s} + z_k, \quad (1)$$

¹Since we focus on the capacity for RIS assisted multicast, we consider the single group scenario (pure multicast), i.e., the BS sends the same message to all K MUs. If this is the multi-group scenario (K MUs divided into multiple groups, and the BS sends an independent message to each group), we need to study the capacity region rather than capacity.

where $\mathbf{s} = [s_1, s_2, \dots, s_M]^T$ is the transmitted symbol vector; $\mathbf{t}_k^H \in \mathbb{C}^{1 \times M}$ is the channel vector between the BS and MU k , i.e., $\mathbf{t}_k^H = [t_{k,1}, t_{k,2}, \dots, t_{k,M}]$, with $t_{t,m} = a_{t,t,m} e^{j\theta_{t,t,m}}$; $\mathbf{H} \in \mathbb{C}^{N \times M}$ is the channel matrix between the BS and the RIS, i.e.,

$$\mathbf{H} = \begin{bmatrix} H_{1,1} & H_{1,2} & \cdots & H_{1,M} \\ H_{2,1} & H_{2,2} & \cdots & H_{2,M} \\ \vdots & \vdots & \ddots & \vdots \\ H_{N,1} & H_{N,2} & \cdots & H_{N,M} \end{bmatrix}, \quad (2)$$

with $H_{n,m} = a_{H_{n,m}} e^{j\theta_{H_{n,m}}}$; $\mathbf{h}_k^H \in \mathbb{C}^{1 \times N}$ is the channel vector between the RIS and the MU k , i.e.,

$$\mathbf{h}_k^H = [h_{k,1}, h_{k,2}, \dots, h_{k,N}], \quad (3)$$

with $h_{k,n} = a_{h_{k,n}} e^{j\theta_{h_{k,n}}}$; $\Phi = \text{diag}[\Phi_1, \Phi_2, \dots, \Phi_N] \in \mathbb{C}^{N \times N}$ represents the phase shifts introduced by the reflecting elements at the RIS, with $\Phi_n = e^{j\theta_n}$; and z_k is the circularly symmetric complex Gaussian (CSCG) noise with zero mean and unit variance $\sigma^2 = 1$.

In fact, it is hard to directly obtain the CSI of the separate BS-RIS and separate RIS-MU links, i.e., \mathbf{H} and \mathbf{h}_k^H . However, the signal model (1) is equivalent to

$$y_k = (\mathbf{u}^H \mathbf{G}_k \mathbf{H} + \mathbf{t}_k^H) \mathbf{s} + z_k, \quad (4)$$

where $\mathbf{G}_k \mathbf{H}$ is the cascaded channel from the BS to the k -th MU via RIS, and $\mathbf{u}^H = [\Phi_1, \dots, \Phi_N]$, $\mathbf{G}_k = \text{diag}(\mathbf{h}_k)$. Notice that the cascaded CSI of the channel matrix $\mathbf{G}_k \mathbf{H}$ can be acquired to the BS, which implies that the each element of matrix $\mathbf{G}_k \mathbf{H}$, i.e., $h_{k,n} H_{n,m} = a_{h_{k,n}} a_{H_{n,m}} e^{j(\theta_{h_{k,n}} + \theta_{H_{n,m}})}$, is known.

B. Problem Formulation

For the fixed Φ , the capacity of RIS assisted multicast channel is given by [32], [33]

$$C(\Phi) \triangleq \max_{\mathbf{Q}: \mathbf{Q} \succeq 0, \text{Tr}(\mathbf{Q}) \leq P_{\max}} \min_{k=1, \dots, K} \log \left[1 + (\mathbf{u}^H \mathbf{G}_k \mathbf{H} + \mathbf{t}_k^H) \mathbf{Q} (\mathbf{H}^H \mathbf{G}_k^H \mathbf{u} + \mathbf{t}_k) \right] \quad (5)$$

where $\mathbf{Q} = \mathbb{E}\{\mathbf{s}\mathbf{s}^H\}$ is the covariance matrix of the transmitted symbol vector \mathbf{s} ; P_{\max} is the power budget, and $\text{Tr}(\mathbf{Q}) \leq P_{\max}$ is the power constraint. From (5), it is observed that the capacity depends on Φ . In order to obtain the optimal capacity for the equivalent multicast channel by jointly the optimizing the covariance matrix \mathbf{Q} and the phase shifts $\theta = [\theta_1, \theta_2, \dots, \theta_N]^T$, an optimization problem is formulated as

$$(\text{P1})C = \max_{\mathbf{Q}, \theta} \min_{k=1, \dots, K} \log \left[1 + (\mathbf{u}^H \mathbf{G}_k \mathbf{H} + \mathbf{t}_k^H) \mathbf{Q} (\mathbf{H}^H \mathbf{G}_k^H \mathbf{u} + \mathbf{t}_k) \right] \quad (6)$$

$$\text{s.t. } \text{Tr}(\mathbf{Q}) \leq P_{\max}, \quad (7)$$

$$\mathbf{Q} \succeq 0, \quad (8)$$

$$|\Phi_n| = 1, n = 1, 2, \dots, N. \quad (9)$$

Since the objective function in (6) is non-convex due to the phase shifts [34], Problem (P1) is non-convex, and its

optimal solution cannot be obtained directly by any effective and standard method. Moreover, the objective function (6) is non-differentiable because the pointwise minimum $\min\{\cdot\}$ is non-differentiable [34], and hence the KKT conditions² for (P1) do not exist [34].

III. PROPOSED ALGORITHM TO PROBLEM (P1)

In this section, we propose two efficient algorithms to find the phase shifts and covariance matrix for Problem (P1). First, the objective function in (6) for Problem (P1) is non-differentiable, and thus we reformulate (P1) as the following differentiable problem:

$$(P2) \max_{\mathbf{Q}, \boldsymbol{\theta}, \gamma} \gamma \quad (10)$$

$$\begin{aligned} \text{s.t. } & \gamma \leq (\mathbf{u}^H \mathbf{G}_k \mathbf{H} + \mathbf{t}_k^H) \mathbf{Q} (\mathbf{H}^H \mathbf{G}_k^H \mathbf{u} + \mathbf{t}_k), \\ & k = 1, \dots, K, \\ & (7), (8), (9), \end{aligned} \quad (11)$$

where γ is an auxiliary variable. Notice that Problems (P1) and (P2) have the same optimal solution $\{\mathbf{Q}_*, \boldsymbol{\theta}_*\}$. In this section, we propose two algorithms, i.e., gradient descent method and alternating optimization to obtain the locally optimal solution for (P2).

Since (P2) is an inequality constrained optimization problem and continuously differentiable, we perform the logarithmic barrier method, which is one of the descent methods [34], to converge the objective function of (P2) as a local optimum.

A. Gradient Descent Method

We reformulate Problem (P2) as an unconstrained minimization problem

$$(P2-t) \min \Gamma^{(t)}(\mathbf{Q}, \boldsymbol{\theta}, \gamma), \quad (12)$$

where $\Gamma^{(t)}(\mathbf{Q}, \boldsymbol{\theta}, \gamma) = -\gamma - \frac{1}{t} f(\mathbf{Q}, \boldsymbol{\theta}, \gamma)$, and $f(\mathbf{Q}, \boldsymbol{\theta}, \gamma)$ is given as

$$\begin{aligned} f(\mathbf{Q}, \boldsymbol{\theta}, \gamma) = & \sum_{k=1}^K \log(-\gamma + (\mathbf{u}^H \mathbf{G}_k \mathbf{H} + \mathbf{t}_k^H) \\ & \mathbf{Q} (\mathbf{H}^H \mathbf{G}_k^H \mathbf{u} + \mathbf{t}_k)) + \log(-\text{Tr}(\mathbf{Q}) \\ & + P_{\max}) + \log(\det \mathbf{Q}), \end{aligned} \quad (13)$$

and $-\frac{1}{t} \log(-x)$ is the logarithmic barrier function for the inequality constraints.

Problem (P2-t) can be regarded as an approximation of Problem (P2), where $t > 0$ is a parameter to the accuracy of the approximation. Thus, a large value of t can be used to approximate Problem (P2).

We solve a sequence of problems with each corresponding to (P2-t) for a certain value of t sorted in ascending order, and the optimal point for the previous problem in the sequence is used as the initial value for the current one [34].

For Problem (P2-t), we perform the gradient descent method to compute the optimal solution $\{\mathbf{Q}^{(t)}, \boldsymbol{\theta}^{(t)}, \gamma^{(t)}\}$,

where the descent direction $\{\Delta \mathbf{Q}, \Delta \boldsymbol{\theta}, \Delta \gamma\}$ and the step size k are obtained as follows.

- **Descent Direction:** By taking the derivative of $\Gamma^{(t)}(\mathbf{Q}, \boldsymbol{\theta}, \gamma)$ with respect to \mathbf{Q} , $\boldsymbol{\theta}$, and γ , respectively, we obtain the descent direction as

$$\begin{aligned} \Delta \mathbf{Q} = & \frac{1}{t} \sum_{k=1}^K \frac{(\mathbf{H}^H \mathbf{G}_k^H \mathbf{u} + \mathbf{t}_k) (\mathbf{u}^H \mathbf{G}_k \mathbf{H} + \mathbf{t}_k^H)}{-\gamma + (\mathbf{u}^H \mathbf{G}_k \mathbf{H} + \mathbf{t}_k^H) \mathbf{Q} (\mathbf{H}^H \mathbf{G}_k^H \mathbf{u} + \mathbf{t}_k)} \\ & + \frac{\mathbf{I}}{t(\text{Tr}(\mathbf{Q}) - P_{\max})} + \frac{\mathbf{Q}^{-1}}{t}, \end{aligned} \quad (14)$$

$$\Delta \boldsymbol{\theta} = \frac{1}{t} \sum_{k=1}^K \frac{(\mathbf{G}_k \mathbf{H} \mathbf{Q} \mathbf{H}^H \mathbf{G}_k^H + 2\mathbf{t}_k^H \mathbf{Q} \mathbf{H}^H \mathbf{G}_k^H) \boldsymbol{\varphi}}{-\gamma + (\mathbf{u}^H \mathbf{G}_k \mathbf{H} + \mathbf{t}_k^H) \mathbf{Q} (\mathbf{H}^H \mathbf{G}_k^H \mathbf{u} + \mathbf{t}_k)}, \quad (15)$$

$$\Delta \gamma = 1 - \frac{1}{t} \sum_{k=1}^K \frac{1}{-\gamma + (\mathbf{u}^H \mathbf{G}_k \mathbf{H} + \mathbf{t}_k^H) \mathbf{Q} (\mathbf{H}^H \mathbf{G}_k^H \mathbf{u} + \mathbf{t}_k)}. \quad (16)$$

where $\boldsymbol{\varphi} = [je^{j\theta_1}, \dots, je^{j\theta_N}]^T$.

- **Step Size:** We also adopt the backtracking line search to determine the step size k , where the initial value of k is $k = 1$ and then the value of k is reduced by $k := k\eta$, with $0 < \eta < 1$, until the stopping condition

$$\begin{aligned} \Gamma^{(t)}(\mathbf{Q} + k\Delta \mathbf{Q}, \boldsymbol{\theta} + k\Delta \boldsymbol{\theta}, \gamma + k\Delta \gamma) < \Gamma^{(t)} \\ (\mathbf{Q}, \boldsymbol{\theta}, \gamma) - \alpha k (\|\Delta \mathbf{Q}\|_{m_2}^2 + \|\Delta \boldsymbol{\theta}\|^2 + |\Delta \gamma|^2) \end{aligned} \quad (17)$$

satisfies.

Algorithm Summary: Based on the above discussion, we can compute the optimal solution $\{\mathbf{Q}_*, \boldsymbol{\theta}_*, \gamma_*\}$ for Problem (P2) by two-level iterations, and the detailed algorithm is summarized in Algorithm 1.

From (17), it follows that $\Gamma^{(t)}(\mathbf{Q}, \boldsymbol{\theta})$ decreases over iterations. Thus, Algorithm 1 is guaranteed to converge to a locally optimal solution. The convergence rate of the Algorithm 1 is at least linear form [34].

From [35], we obtain that the complexity of each iteration is mainly due to the calculations of $\Delta \mathbf{Q}$ and $\Delta \boldsymbol{\theta}$, whose complexities are $\mathcal{O}((MN^2 + M^2N)K + M^3)$ [35] and $\mathcal{O}(N^2 + M^2 + MN)$. It is obvious that the order of the complexity of $\Delta \boldsymbol{\theta}$ is less than that of $\Delta \mathbf{Q}$, we can ignore the complexity of $\Delta \boldsymbol{\theta}$. Then, the number of the inner and outer iterations are I and J , respectively, and thus the complexity of Algorithm 1 is given as $\mathcal{O}(((MN^2 + M^2N)K + M^3)IJ)$ [35].

B. Alternating Optimization

If we only optimize \mathbf{Q} for Problem (P2), the corresponding subproblem is convex. Thus, we consider adopting the alternating optimization technique to separately and iteratively solve for \mathbf{Q} and $\boldsymbol{\theta}$. In each iteration, we first optimize \mathbf{Q} with fixed $\boldsymbol{\theta}$, and then solve for $\boldsymbol{\theta}$ with fixed \mathbf{Q} . For the phase shift optimization problem, the non-convex constraints (11) are handled by the characteristic of multicast capacity expression, and then we obtain the optimal semi-closed form solution.

²KKT conditions are the necessary conditions that optimal solutions need to satisfy for a differentiable problem.

Algorithm 1 Gradient Descent Method for Problem (P2)

Input: $\mathbf{G}_k, k = 1, \dots, K, \mathbf{H}, P_{\max}$, and the error tolerances $\delta_1 > 0$ and $\delta_2 > 0$.

Output: $\{\mathbf{Q}_*, \boldsymbol{\theta}_*, \gamma_*\}$.

- 1: **Initialize** $\{\mathbf{Q}^{(t_i)}, \boldsymbol{\theta}^{(t_i)}, \gamma^{(t_i)}\}$ and $\{\mathbf{Q}_j, \boldsymbol{\theta}_j, \gamma_j\}$, which represent the output of the i -th outer iteration and the input of the j -th inner iteration, respectively.
- 2: **while** $\frac{1}{t_{i-1}} > \delta_1$ **do**
- 3: Let $t_i = \rho t_{i-1}$.
- 4: **Initialize** $\mathbf{Q} = \mathbf{Q}^{(t_{i-1})}$, $\boldsymbol{\theta} = \boldsymbol{\theta}^{(t_{i-1})}$, and $\gamma^{(t_{i-1})}$.
- 5: **while** $|\Gamma^{(t_i)}(\mathbf{Q}_j, \boldsymbol{\theta}_j, \gamma_j) - \Gamma^{(t_i)}(\mathbf{Q}_{j-1}, \boldsymbol{\theta}_{j-1}, \gamma_{j-1})| > \delta_2$ **do**
- 6: Compute $\Delta \mathbf{Q}_{j+1}$, $\Delta \boldsymbol{\theta}_{j+1}$, and $\Delta \gamma_{j+1}$ by (14), (15) and (16), respectively.
- 7: **Initialize** $l_1 = l_0$
- 8: **while** Condition (17) is false **do**
- 9: Let $l_i := l_{i-1}\eta$.
- 10: **end while**
- 11: Let $\mathbf{Q}_{j+1} = \mathbf{Q}_j + l_i \Delta \mathbf{Q}_{j+1}$, $\boldsymbol{\theta}_{j+1} = \boldsymbol{\theta}_j + l_i \Delta \boldsymbol{\theta}_{j+1}$, and $\gamma_{j+1} = \gamma_j + l_i \Delta \gamma_{j+1}$.
- 12: **end while**
- 13: Let $\mathbf{Q}^{(t_i)} = \mathbf{Q}_{j+1}$, $\boldsymbol{\theta}^{(t_i)} = \boldsymbol{\theta}_{j+1}$, and $\gamma^{(t_i)} = \gamma_{j+1}$.
- 14: **end while**
- 15: Let $\{\mathbf{Q}_*, \boldsymbol{\theta}_*, \gamma_*\} = \{\mathbf{Q}^{(t_i)}, \boldsymbol{\theta}^{(t_i)}, \gamma^{(t_i)}\}$.

1) *Optimization of \mathbf{Q} With Fixed $\boldsymbol{\theta}$:* For the fixed $\boldsymbol{\theta}$, the subproblem which only optimizes \mathbf{Q} is formulated as

$$(P2.1) \max_{\mathbf{Q}, \gamma} \gamma \quad (18)$$

$$\text{s.t. } \gamma \leq \text{Tr}(\mathbf{R}_k \mathbf{Q}), k = 1, \dots, K \quad (19)$$

$$(7), (8),$$

where $\mathbf{R}_k = (\mathbf{H}^H \mathbf{G}_k^H \mathbf{u} + \mathbf{t}_k)(\mathbf{u}^H \mathbf{G}_k \mathbf{H} + \mathbf{t}_k^H)$, and (19) is due to

$$(\mathbf{u}^H \mathbf{G}_k \mathbf{H} + \mathbf{t}_k^H) \mathbf{Q} (\mathbf{H}^H \mathbf{G}_k^H \mathbf{u} + \mathbf{t}_k) = \text{Tr}(\mathbf{R}_k \mathbf{Q}). \quad (20)$$

Obviously, Problem (P2) is a convex problem and can be efficiently solved by standard semi-definite programming (SDP) [34] and we can employ standard convex optimization tools, e.g., CVX [36], to compute the optimal solution.

2) *Optimization of $\boldsymbol{\theta}$ With Fixed \mathbf{Q} :* Next, we solve the following subproblem with the fixed \mathbf{Q} :

$$(P2.2) \max_{\boldsymbol{\theta}, \gamma} \gamma \quad (21)$$

$$\text{s.t. } (9), (11).$$

Since \mathbf{Q} is a positive semi-definite matrix, the eigenvalue decomposition of $\mathbf{U} \boldsymbol{\Sigma} \mathbf{U}^H$ can be obtained, where $\mathbf{U} \in \mathbb{C}^{M \times M}$, and diagonal elements in $\boldsymbol{\Sigma}$ are non-negative real numbers. Thus, we can define $\mathbf{V} = \mathbf{H} \mathbf{U} \boldsymbol{\Sigma}^{\frac{1}{2}} = [\mathbf{v}_1, \dots, \mathbf{v}_N]^H \in \mathbb{C}^{N \times M}$ and $\mathbf{p}_k = \boldsymbol{\Sigma}^{\frac{1}{2}} \mathbf{U}^H \mathbf{t}_k \in \mathbb{C}^{M \times 1}$. Then, $(\mathbf{u}^H \mathbf{G}_k \mathbf{H} + \mathbf{t}_k^H) \mathbf{Q} (\mathbf{H}^H \mathbf{G}_k^H \mathbf{u} + \mathbf{t}_k)$ in (11) can be rewritten as

$$\begin{aligned} & (\mathbf{u}^H \mathbf{G}_k \mathbf{H} + \mathbf{t}_k^H) \mathbf{Q} (\mathbf{H}^H \mathbf{G}_k^H \mathbf{u} + \mathbf{t}_k) \\ &= \mathbf{u}^H \mathbf{G}_k \mathbf{V} \mathbf{V}^H \Phi^H \mathbf{t}_k + \mathbf{u}^H \mathbf{G}_k \mathbf{V} \mathbf{p}_k \\ & \quad + \mathbf{p}_k^H \mathbf{V}^H \mathbf{G}_k^H \mathbf{u} + \mathbf{t}_k^H \mathbf{Q} \mathbf{t}_k \end{aligned}$$

$$\begin{aligned} &= \sum_{i=1}^N e^{j\theta_i} h_{k,i} \mathbf{v}_i^H \sum_{j=1}^N e^{-j\theta_j} h_{k,j}^* \mathbf{v}_j + \sum_{i=1}^N e^{j\theta_i} h_{k,i} \mathbf{v}_i^H \mathbf{p}_k \\ & \quad + \sum_{j=1}^N e^{-j\theta_j} h_{k,j}^* \mathbf{p}_k^H \mathbf{v}_j + \mathbf{t}_k^H \mathbf{Q} \mathbf{t}_k \\ &= \sum_{n=1}^N |h_{k,n}|^2 \mathbf{v}_n^H \mathbf{v}_n + \sum_{i=1}^N \sum_{j=1, j \neq i}^N e^{j(\theta_i - \theta_j)} h_{k,i} h_{k,j}^* \mathbf{v}_i^H \mathbf{v}_j \\ & \quad + \sum_{i=1}^N 2c_{i,k} \cos(\theta_i + \omega_{i,k}) + \mathbf{t}_k^H \mathbf{Q} \mathbf{t}_k \\ &= a_k + \sum_{i=1}^N \sum_{j=i+1}^N 2b_{i,j,k} \cos(\theta_i - \theta_j + \psi_{i,j,k}) \\ & \quad + \sum_{i=1}^N 2c_{i,k} \cos(\theta_i + \omega_{i,k}), \quad (22) \end{aligned}$$

where $a_k = \sum_{n=1}^N |h_{k,n}|^2 \mathbf{v}_n^H \mathbf{v}_n + \mathbf{t}_k^H \mathbf{Q} \mathbf{t}_k$, $b_{i,j,k} = |h_{k,i} h_{k,j}^* \mathbf{v}_i^H \mathbf{v}_j|$, $c_{i,k} = |t_{k,i} \mathbf{v}_i^H \mathbf{p}_k|$, $\psi_{i,j,k} = \arg(h_{k,i} h_{k,j}^* \mathbf{v}_i^H \mathbf{v}_j)$, $\omega_{i,k} = \arg(h_{k,i} \mathbf{v}_i^H \mathbf{p}_k)$ are constants. From (22), it follows that the condition (11) in Problem (P2.2) can be simplified as

$$\begin{aligned} \gamma \leq a_k + \sum_{i=1}^N \sum_{j=i+1}^N 2b_{i,j,k} \cos(\theta_i - \theta_j + \psi_{i,j,k}) \\ + \sum_{i=1}^N 2c_{i,k} \cos(\theta_i + \omega_{i,k}), k = 1, \dots, K \quad (23) \end{aligned}$$

Based on (23), we can obtain the semi-closed-form solution for Problem (P2.2) can be obtained as the following proposition.

Proposition 1: The necessary conditions that the optimal solution $\{\boldsymbol{\theta}_Q, \gamma^*\}$ of Problem (P2-2) needs to satisfy are given as (23) and

$$\begin{aligned} \lambda_k \left(\gamma - a_k - \sum_{i=1}^N \sum_{j=i+1}^N 2b_{i,j,k} \cos(\theta_i - \theta_j + \psi_{i,j,k}) \right. \\ \left. - \sum_{i=1}^N 2c_{i,k} \cos(\theta_i + \omega_{i,k}) \right) = 0, \\ \sum_{j=1, j \neq n}^N \bar{b}_{n,j} \sin(\theta_n - \theta_j + \bar{\psi}_{n,j}) + \bar{c}_n \sin(\theta_n + \bar{\omega}_n) = 0, \\ n = 1, \dots, N, -1 + \sum_{k=1}^K \lambda_k = 0, \\ k = 1, \dots, K, \quad (24) \end{aligned}$$

where $\bar{b}_{n,j} = \sum_{k=1}^K 2\lambda_k b_{n,j,k}$, $\bar{c}_n = \sum_{k=1}^K 2\lambda_k c_{n,k}$, $\bar{\psi}_{n,j}$ and $\bar{\omega}_n$ are the auxiliary angle of $\psi_{n,j,k}$ and $\omega_{n,k}$, $k = 1, \dots, K$, respectively.

Proof: Lagrangian function of Problem (P2.2) is given as

$$\begin{aligned} L = -\gamma + \sum_{k=1}^K \lambda_k \left[- \sum_{i=1}^N \sum_{j=i+1}^N 2b_{i,j,k} \cos(\theta_i - \theta_j + \psi_{i,j,k}) \right. \\ \left. - \sum_{i=1}^N 2c_{i,k} \cos(\theta_i + \omega_{i,k}) + \gamma - a_k \right]. \quad (25) \end{aligned}$$

Based on [34], we obtain that for the non-convex problem, by taking the derivative of the Lagrangian function (25), we can obtain the KKT optimality conditions in (24), which are the necessary conditions that the optimal solution $\{\theta_{\mathbf{Q}}, \gamma^*\}$ needs to satisfy. ■

We denote the solution set of equation set (24) as Ω , which can be obtained by the interval iterative method [37]. The main ideas of this method are given as follow: First, we divide the domain of θ into a finite number of initial intervals and make sure that each interval has a unique solution (When the radius of the interval is greater than the radius of its Krawczyk operator, the interval has a unique solution). Then, when we make sure each interval only has one solution, we start to obtain the solution via the iteration method. In each iteration, we obtain the intersection of the intervals and the its Krawczyk operator as the new interval, and then compute the new Krawczyk operator of the new interval for the next iteration. Until the radius of the interval is smaller than an error. The center of the interval can be regarded as a solution.

From (21), it is observed that the optimal solution $\{\theta_{\mathbf{Q}}, \gamma^*\}$ can be determined by the maximums of all γ , which belong to set Ω , i.e.,

$$\gamma^* = \max \{\gamma : \{\theta, \gamma\} \in \Omega\}, \quad (26)$$

and the corresponding $\theta_{\mathbf{Q}}$ is optimal for Problem (P2.2).

3) *Algorithm Summary*: The detailed alternating optimization for Problem (P2) is summarized as Algorithm 2. In each iteration, we first optimize \mathbf{Q}_{i+1} with the fixed θ_i , which is obtained at the previous iteration. Then, we optimize θ_{i+1} for the fixed \mathbf{Q}_{i+1} by Proposition 1 and (26), which is obtained at the current iteration.

Algorithm 2 Alternating Optimization for Problem (P2)

Input: \mathbf{G}_k , $k = 1, \dots, K$, \mathbf{H} , P_{\max} , and error tolerances $\delta > 0$.

Output: $\{\mathbf{Q}_*, \theta_*\}$.

- 1: **Initialize** Randomly generate J independent realizations of $\theta^{(j)}$, $j = 1, \dots, J$, and compute the corresponding optimal $\mathbf{Q}^{(j)}$, $j = 1, \dots, J$, according CVX. Select initial value $\{\mathbf{Q}_1, \theta_1\}$ as the realization yielding the largest objective value of Problem (P2)
 - 2: **while** $|\gamma_i - \gamma_{i-1}| > \delta$ **do** as
 - 3: Compute \mathbf{Q}_{i+1} with the fixed θ_i by CVX.
 - 4: Compute θ_{i+1} with the fixed \mathbf{Q}_{i+1} by Proposition 1 and (26).
 - 5: Let $\gamma_{i+1} = \max \{\mathbf{u}^H \mathbf{G}_k \mathbf{H} \mathbf{Q}_{i+1} \mathbf{H}^H \mathbf{G}_k^H \mathbf{u}_{i+1}\}$
 - 6: **end while**
 - 7: Let $\{\mathbf{Q}_*, \theta_*\} = \{\mathbf{Q}_{i+1}, \theta_{i+1}\}$
-

C. Optimal Solution for the Special Case

The previous two subsections proposed two numerical algorithms to obtain the phase shifts and covariance matrix for Problem (P1), which loses insight and cannot obtain the optimal solution for Problem (P1). However, the semi-closed-form optimal solution can be obtained in a special case that we only need to maximize the capacity of a MU. We first show

the sufficient and necessary conditions that the special case happens, and then compute the semi-closed-form optimal solution of the special case.

For the convenience, Problem (P1) can be rewritten as

$$\max_{\{\mathbf{Q}, \theta\} \in \mathcal{Q}} \min_{k=1, \dots, K} R_k(\mathbf{Q}, \theta), \quad (27)$$

where $\mathcal{Q} = \{\mathbf{Q}, \theta | (7), (8), (9)\}$ is the feasible set for Problem (P1), and $R_k(\mathbf{Q}, \theta)$ is defined as

$$R_k(\mathbf{Q}, \theta) = \log(1 + (\mathbf{u}^H \mathbf{G}_k \mathbf{H} + \mathbf{t}_k^H) \mathbf{Q} (\mathbf{H}^H \mathbf{G}_k^H \mathbf{u} + \mathbf{t}_k)). \quad (28)$$

First, the following proposition shows the sufficient and necessary conditions that the special case happens.

Proposition 2: The optimal solution for $\max_{\{\mathbf{Q}, \theta\} \in \mathcal{Q}} R_{k_0}(\mathbf{Q}, \theta)$ is denoted as $\{\mathbf{Q}_{k_0}, \theta_{k_0}\}$, $k_0 \in \{1, \dots, K\}$. If and only if

$$R_{k_0}(\mathbf{Q}_{k_0}, \theta_{k_0}) \leq R_k(\mathbf{Q}_{k_0}, \theta_{k_0}), \quad k = 1, \dots, K, \quad (29)$$

then $\{\mathbf{Q}_{k_0}, \theta_{k_0}\}$ is the optimal solution for Problem (P1).

Proof: The necessary of the conditions (29) is obvious. We only prove the sufficiency of the conditions (29). We denote $\{\mathbf{Q}_*, \theta_*\}$ is the optimal solution for Problem (P1). Due to (29), it follows

$$\begin{aligned} \min_{k=1, \dots, K} R_k(\mathbf{Q}_*, \theta_*) &\leq R_{k_0}(\mathbf{Q}_*, \theta_*) \\ &\leq R_{k_0}(\mathbf{Q}_{k_0}, \theta_{k_0}) \\ &\leq R_k(\mathbf{Q}_{k_0}, \theta_{k_0}), \quad k = 1, \dots, K. \end{aligned} \quad (30)$$

Based on (30), we obtain $\min_{k=1, \dots, K} R_k(\mathbf{Q}_*, \theta_*) \leq \min_{k=1, \dots, K} R_k(\mathbf{Q}_{k_0}, \theta_{k_0})$, which implies that $\{\mathbf{Q}_{k_0}, \theta_{k_0}\}$ is the optimal solution for Problem (P1). ■

Remark 1: From Proposition 2, we observe that in this special case, even if we only maximize the capacity of the MU k_0 , its capacity is still smaller than the capacities of other MUs. In other words, in this special case, even if we optimize channel condition for MU k_0 by designing the phase shift θ , the MU k_0 still own the worst channel condition. It implies that the multicast capacity only depends on the capacity for the MU k_0 .

Next, we show how to obtain $\{\mathbf{Q}_{k_0}, \theta_{k_0}\}$ by optimizing

$$\max_{\{\mathbf{Q}, \theta\} \in \mathcal{Q}} \log(1 + (\mathbf{u}^H \mathbf{G}_{k_0} \mathbf{H} + \mathbf{t}_{k_0}^H) \mathbf{Q} (\mathbf{H}^H \mathbf{G}_{k_0}^H \mathbf{u} + \mathbf{t}_{k_0})), \quad (31)$$

which is equivalent to the capacity of multiple-input single-output (MISO) channel [32]. For the MISO channel, the capacity equals that of a single-input single-output channel with the signal transmitted over the multiple-antenna coherently combined to maximize the channel signal noise ratio (SNR). Thus, for a fixed θ , the corresponding capacity and optimal covariance matrix \mathbf{Q}_θ are respectively given as [32]

$$\begin{aligned} \max_{\mathbf{Q} \in \mathcal{Q}} \log(1 + (\mathbf{u}^H \mathbf{G}_{k_0} \mathbf{H} + \mathbf{t}_{k_0}^H) \mathbf{Q} (\mathbf{H}^H \mathbf{G}_{k_0}^H \mathbf{u} + \mathbf{t}_{k_0})) \\ = \log(1 + P_{\max} \|(\mathbf{u}^H \mathbf{G}_{k_0} \mathbf{H} + \mathbf{t}_{k_0}^H)\|^2), \end{aligned} \quad (32)$$

$$\mathbf{Q}_\theta = \mathbf{V}_\theta^H \text{diag}[P_{\max}, 0, \dots, 0] \mathbf{V}_\theta, \quad (33)$$

where $\mathbf{V}_\theta \in \mathbb{C}^{N \times N}$ is obtained by the singular value decomposition of $\mathbf{u}^H \mathbf{G}_{k_0} \mathbf{H} + \mathbf{t}_{k_0}^H$, i.e.,

$$\mathbf{u}^H \mathbf{G}_{k_0} \mathbf{H} + \mathbf{t}_{k_0}^H \triangleq \mathbf{U}_\theta \Sigma_\theta \mathbf{V}_\theta^H, \quad (34)$$

where $\mathbf{U}_\theta = \mathbf{1}$, \mathbf{V}_θ^H is unitary matrix, and $\Sigma_\theta \in \mathbb{C}^{1 \times N}$ is a rectangular vector whose first element are non-negative real numbers and whose other elements are zero.

Remark 2: From (32), (33) and (34), it is observed that we only need to compute θ_0 for maximizing $\log \left(1 + P_{\max} \left\| \left(\mathbf{u}^H \mathbf{G}_{k_0} \mathbf{H} + \mathbf{t}_{k_0}^H \right) \right\|^2 \right)$. After θ_0 is obtained, \mathbf{Q}_{k_0} can be obtained by (33) and (34).

Thus, we only need to solve the following problem

$$(P3) \max_{\theta} \left\| \left(\mathbf{u}^H \mathbf{G}_{k_0} \mathbf{H} + \mathbf{t}_{k_0}^H \right) \right\|^2. \quad (35)$$

Then, the optimal solution θ_{k_0} for Problem (P3) is summarized in the following proposition.

Proposition 3: The necessary conditions for the optimal solution $\theta_{k_0} = [\theta_{k_0,1}, \dots, \theta_{k_0,N}]$ for Problem (P3) are given as

$$\begin{aligned} 0 &= \sum_{m=1}^M \sum_{j=1, j \neq n}^N 2G_{n,j,m}^{(2)} \sin \left(\theta_{k_0,n} - \theta_{k_0,j} + \vartheta_{n,j,m}^{(2)} \right) \\ &+ \sum_{m=1}^M 2B_{n,m}^{(2)} \sin \left(\theta_{k_0,n} + \iota_{n,m} \right), \end{aligned} \quad (36)$$

where $G_{n,j,m}^{(2)} = a_{h_{2,n}} a_{H_{n,m}} a_{h_{2,j}} a_{H_{j,m}}$, $\vartheta_{n,j,m}^{(2)} = \theta_{h_{2,n}} + \theta_{H_{n,m}} - \theta_{h_{2,j}} - \theta_{H_{j,m}}$, $B_{n,m}^{(2)} = a_{h_{2,n}} a_{H_{n,m}} a_{t_{2,m}}$, and $\iota_{n,m} = \theta_{h_{2,n}} + \theta_{H_{n,m}} + \theta_{t_{2,m}}$.

Proof: Same as Proposition 1, and hence omitted for simplicity. ■

Remark 3: From Proposition 3, we have

- The solution set \mathcal{Q} which satisfies condition (36) can be obtained by the interval iterative method [37]. The optimal solution θ_{k_0} can be determined by the maximums of all $\Upsilon(\theta)$, where θ belongs to set \mathcal{Q} , i.e.,

$$\Upsilon^*(\theta_{k_0}) = \max \{ \Upsilon(\theta) : \theta \in \mathcal{Q} \}, \quad (37)$$

where

$$\begin{aligned} \Upsilon(\theta) &= \sum_{m=1}^M \sum_{i=1}^N \sum_{j=i+1}^N 2G_{i,j,m}^{(2)} \cos \left(\theta_i - \theta_j + \vartheta_{i,j,m}^{(2)} \right) \\ &+ \sum_{m=1}^M \sum_{n=1}^N 2B_{n,m}^{(2)} \cos \left(\theta_n + \iota_{n,m} \right). \end{aligned} \quad (38)$$

If the special case happens, we adopt (37) to obtain the optimal solution; else we adopt the gradient descent method and alternating optimization to solve Problem (P2).

- Proposition 3 only presents the semi-closed-form optimal solution for Problem (P3). Here, we set $M = 1$ for example to demonstrate Proposition 3 for (P3), which has the closed-form solutions.

When $M = 1$, (P3) can be rewritten as

$$\begin{aligned} \max_{\theta} & \sum_{i=1}^N \sum_{j=i+1}^N 2G_{i,j,1}^{(2)} \cos \left(\theta_{k_0,i} - \theta_{k_0,j} + \vartheta_{i,j,1}^{(2)} \right) \\ & + \sum_{i=1}^N 2B_{i,1}^{(2)} \cos \left(\theta_{k_0,i} + \iota_{i,1} \right). \end{aligned} \quad (39)$$

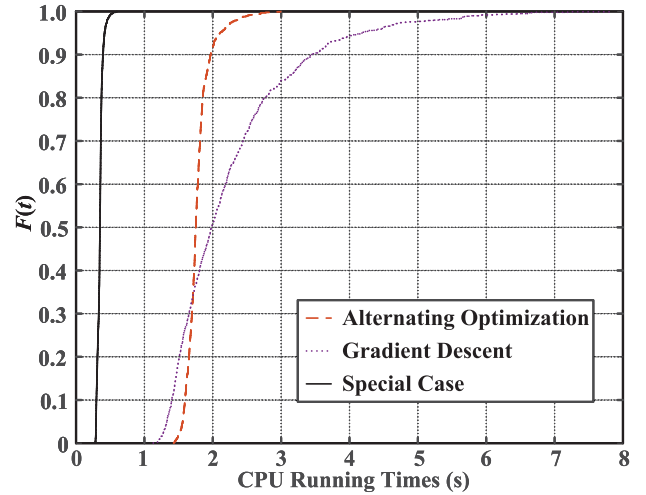


Fig. 2. The cumulative distribution function of running times.

Therefore, $\theta_{k_0,n} = -(\theta_{h_{2,n}} + \theta_{H_{n,1}} + \theta_{t_{2,1}})$, $n = 1, \dots, N$, is optimal for (39), which is the optimal solution for $M = 1$ as well.

Fig. 2 shows the cumulative distribution function of running times under the gradient descent, the alternating optimization, and the special case, where $\rho = 20$ (dB), $N = 8$, and $M = 8$. It is observed that the running time of the special case is smaller than those of gradient descent and the alternating optimization.

IV. ASYMPTOTIC ANALYSIS

In the previous two sections, the capacity of RIS assisted multicast transmission is maximized by the numerical algorithms, which lose some intuition for the performance of RIS in multicast transmission. Since the reflecting elements are low-cost with a simple structure, the RIS can integrate a large number of the reflecting elements [13]. Thus, it is worth to study the asymptotic behaviors of capacity C when some or all of the number of reflecting elements, BS antennas, and MUs go to infinity. We consider \mathbf{H} , \mathbf{G}_k^H , and \mathbf{t}_k^H as Rician Fading. The channels of the BS-RIS link, the RIS-MUs links, and the BS-MUs links are denoted as $\mathbf{H} = \sqrt{\frac{B}{B+1}} \bar{\mathbf{H}} + \sqrt{\frac{1}{B+1}} \hat{\mathbf{H}}$, $\mathbf{G}_k = \sqrt{\frac{B}{B+1}} \text{diag}(\bar{\mathbf{h}}_k) + \sqrt{\frac{1}{B+1}} \text{diag}(\hat{\mathbf{h}}_k)$, and $\mathbf{t}_k = \sqrt{\frac{B}{B+1}} \bar{\mathbf{t}}_k + \sqrt{\frac{1}{B+1}} \hat{\mathbf{t}}_k$, respectively. Here, B is the Rician factor; $\bar{\mathbf{H}}$, $\hat{\mathbf{h}}_k$, and $\hat{\mathbf{t}}_k$ are the non-line-of-sight (NLoS) component, and elements of $\bar{\mathbf{H}}$, $\hat{\mathbf{h}}_k$, and $\hat{\mathbf{t}}_k$ are i.i.d., complex Gaussian distribution $\mathcal{CN}(0, 1)$. The line-of-sight (LoS) components are expressed by uniform rectangular array (URA). The array response of URA is given as $\mathbf{a}_M^H(\omega, \vartheta) = \text{vec}(\mathbf{a}_{M_1}(\omega, \vartheta) \mathbf{a}_{M_2}^H(\omega, \vartheta))$, where $\mathbf{a}_{M_1} = [1, e^{j2\pi \frac{\omega}{\lambda} \sin \omega \cos \vartheta}, \dots, e^{j2\pi \frac{\omega}{\lambda} (M_1-1) \sin \omega \cos \vartheta}]$, $\mathbf{a}_{M_2} = [1, e^{j2\pi \frac{\omega}{\lambda} \sin \omega \sin \vartheta}, \dots, e^{j2\pi \frac{\omega}{\lambda} (M_1-1) \sin \omega \sin \vartheta}]$; ω and ϑ are the angle of departure (AoD) or angle of arrival (AoA) for x-axis and y-axis. Thus, the LoS components $\bar{\mathbf{H}}$, $\bar{\mathbf{h}}_k^H$, and $\bar{\mathbf{t}}_k^H$ are expressed as $\bar{\mathbf{H}} = \mathbf{a}_N(\omega_{AoA}, \vartheta_{AoA}) \mathbf{a}_M^H(\omega_{AoD}, \vartheta_{AoD})$,

$\bar{\mathbf{h}}_k = \mathbf{a}_N(\omega_{AoD}, \vartheta_{AoD})$, and $\bar{\mathbf{t}}_k = \mathbf{a}_M(\omega_{AoD}, \vartheta_{AoD})$, respectively, where ω_{AoA} and ϑ_{AoD} are AoA, and ω_{AoA} and ϑ_{AoA} are the AoD, respectively; d and λ are the antenna separation and wavelength, respectively.

A. Fixed MUs, Increasing Antennas and Reflecting Elements

First, we consider the asymptotic behaviors of the maximal capacity C at the cases where the number of MUs is fixed while either the number of reflecting elements or that of BS antennas goes to infinity.

Proposition 4: If K is fixed, the order growth of C is given as follows.

- When N is fixed and M goes to infinity, C grows at the following rate

$$C \approx \mathcal{O}(\log M). \quad (40)$$

- When M is fixed and N goes to infinity, C grows at the following rate

$$C \approx \mathcal{O}(\log N^2). \quad (41)$$

- When both of N and M go to infinity, C grows at the following rate

$$C \approx \mathcal{O}(\log(N^2M)). \quad (42)$$

Proof: Please see Appendix I. ■

Remark 4: From Proposition 4, we observe

- C grows logarithmically with N^2 and M , as either the number of reflecting elements or that of BS antennas goes to infinity. It follows that the increase in the numbers of antennas and reflecting elements can improve the capacity. This is due to the fact that the diversity order increases as N and M . Moreover, the increase in N can provide more performance gain than that of M . This is due to the fact that with increasing of N , the RIS can provide more the transmit diversity and the receive diversity. The simulations in Fig. 3 also confirms the results in Proposition 4.
- From the results of Proposition 4, we observed that C goes to infinity. In reality, C will converge to a finite value even if N and M go to infinity since the power budget is limited. The main reason for this result is that the Rician channel model assumption is ideal. For Proposition 4.1, we focus on observing the tendency of capacity.
- From the proof of Proposition 4, it is obtained that $C \approx \mathcal{O}\left(\log\left(\frac{B}{B+1}\right)^2\right)$, when B goes to infinity.
- The results in Proposition 4 are under the i.i.d. channel coefficients. However, in some scenarios, the channel coefficients may not be i.i.d., and it leads that the covariances between $g_{k,n,m}$ and $\bar{g}_{k,i,m}$ are not zero. Thus, in the proof of Proposition 4, (75) is rewritten as

$$\begin{aligned} \mathbb{E}\left\{|\Psi_{m,k}|^2\right\} &= A(N^2) + \sum_{n=1}^N \sum_{i=1, i \neq n}^N \\ \mathbf{Cov}(g_{k,n,m}, \bar{g}_{k,i,m}) &\leq A(N^2) \\ &+ N(N-1) \left(1 - \left(\frac{B}{B+1}\right)^2\right). \end{aligned} \quad (43)$$

By the same idea as proof of Proposition 4 and Birkhoff's ergodic theory, we obtain that (40), (41), and (42) are rewritten as

$$C \leq \mathcal{O}(\log N^2) \quad (44)$$

$$C \leq \mathcal{O}(\log M) \quad (45)$$

$$C \leq \mathcal{O}(\log(N^2M)), \quad (46)$$

respectively.

B. Increasing MUs, Fixed Antennas and Reflecting Elements

Then, we consider the asymptotic behaviors of the maximal capacity C at the case where the number of MUs K goes to infinity while both of N and M are fixed. We can see that $\min_{k=1, \dots, K} \{\|\mathbf{h}_k^H\|\} \rightarrow 0$ and $\min_{k=1, \dots, K} \{\|\mathbf{t}_k^H\|\} \rightarrow 0$, as $K \rightarrow \infty$, which implies that at least one RIS-MU link and at least one BS-MU link both being completely unavailable, and we also have $C \rightarrow 0$, which is discussed in detail as follows.

Proposition 5: When both of N and M are fixed, and K goes to infinity, the maximal capacity C goes to 0 at the following rate

$$C \approx \mathcal{O}\left(\frac{1}{K^{1/(N^2M)}}\right). \quad (47)$$

Proof: From the proof of Proposition 4, we obtain that $\|\mathbf{u}^H \mathbf{G}_k \mathbf{H} + \mathbf{t}_k^H\|^2$ follows the non-central chi-square distribution with a mean of $MA(N^2)$ and $2M$ degrees of freedom. It is concluded that the minimum of K non-central chi-squared random variables $\|\mathbf{u}^H \mathbf{G}_k \mathbf{H} + \mathbf{t}_k^H\|^2$, i.e., $\min_{k=1, \dots, K} \{\|\mathbf{u}^H \mathbf{G}_k \mathbf{H} + \mathbf{t}_k^H\|^2\}$, can be scaled as $K^{-1/(MA(N^2))}$ [32].

Note that C is upper bounded by the minimum of the point-to-point capacity of the RIS system as:

$$\begin{aligned} C &\leq \log\left(1 + P_{\max} \min_{k=1, \dots, K} \|\mathbf{u}^H \mathbf{G}_k \mathbf{H} + \mathbf{t}_k^H\|^2\right) \\ &\approx \log\left(1 + \frac{P_{\max}}{K^{1/(MA(N^2))}}\right) \\ &\approx \frac{P_{\max}}{K^{1/(MA(N^2))}}, \end{aligned} \quad (48)$$

which is $\mathcal{O}\left(\frac{1}{K^{1/(N^2M)}}\right)$, and C is lower bounded by the spatially white rate [32]:

$$\begin{aligned} C &\geq \log\left(1 + \frac{P_{\max}}{N} \min_{k=1, \dots, K} \|\mathbf{u}^H \mathbf{G}_k \mathbf{H} + \mathbf{t}_k^H\|^2\right) \\ &\approx \frac{P_{\max}}{NK^{1/(MA(N^2))}}, \end{aligned} \quad (49)$$

which is also $\mathcal{O}\left(\frac{1}{K^{1/(N^2M)}}\right)$. ■

From Proposition 5, it is obtained that C is the inverse proportion with the number of MUs K . The declining ratio decreases with the increasing M and N . It implies that the increase in the M and N can reduce the negative effect of the number of MUs. This result in Proposition 5 has been confirmed in Fig. 5.

C. Increasing MUs, Antennas and Reflecting Elements

Finally, we consider the asymptotic behaviors of the maximal capacity C at the case where all of N , M and K go to infinity.

Proposition 6: When both M and K go to infinity at the ratio $0 < \frac{M}{K} < \infty$, the order growth of C is given as follows:

- If N is fixed, we have

$$\mathbb{E}\{C\} \approx \mathcal{O}(1). \quad (50)$$

- If N goes to infinity, we have

$$\mathcal{O}(1) \leq \mathbb{E}\{C\} \leq \mathcal{O}(\log(N^2)). \quad (51)$$

Proof: See Appendix II. ■

From Proposition 6, we observe the following results. When the number of reflecting elements N is fixed, $\mathbb{E}\{C\}$ remains constant as the number of MUs and antennas are taken to infinity at a fixed ratio. When N goes to infinity, $\mathbb{E}\{C\}$ is lower bounded by a constant, and its growth rate is not greater than $\log N^2$. The above results conclude that increasing the numbers of reflecting elements and antennas can effectively counter the negative effect caused by the increase in MUs. These results are verified by Fig. 6.

From the proof of Proposition 6, we can observe that this proof is not dependent on i.i.d. channel assumption. Thus, the results in Proposition 6 are applicable to non-i.i.d. channel.

V. NUMERICAL RESULTS

This section presents the numerical results of capacity by the following two algorithms: 1) the gradient descent method, 2) alternating optimization. The channel model is same to section IV. Moreover, we set $\rho = \frac{P_{\max}}{\sigma^2}$, $M = 16$, $\frac{d}{\lambda} = 1$, ω_{AoD} , ϑ_{AoD} , ϑ_{AoA} , and ϑ_{AoD} are randomly set within $[0, 2\pi)$. The following numerical results are averaged over 1000 random realization.

A. Benchmark

In comparison, we compute the multicast capacity with the following scheme:

1) *Brute-Force Search:* The optimal solution for Problem (P1) is obtained by brute-force search.

2) *Lower Bound:* The lower bounds of the capacity are obtained by asymptotic analysis.

3) *Beamforming Design:* The covariance matrix \mathbf{Q} degenerates to beamforming vector \mathbf{v} . The capacity in Problem (P1) is rewritten as

$$\max_{\|\mathbf{v}\|^2 \leq P_{\max}} \min_{k=1, \dots, K} \log \left(1 + \|(\mathbf{u}^H \mathbf{G}_k \mathbf{H} + \mathbf{t}_k^H) \mathbf{v}\|^2 \right). \quad (52)$$

The solution is given in [31] in detail.

4) *Beamforming Design With Imperfect CSI:* ³Due to the imperfect cascaded CSI of BS-RIS-MU links, the cascaded

³The beamforming design with imperfect CSI has been studied for the RIS-assisted broadcast transmission. However, there are not works considering the problem for the multicast transmission. This is because this solution of the problem for the multicast transmission is similar to that for the broadcast transmission. Thus, we regard the achievable rate for beamforming design with imperfect CSI as a baseline.

channel $\mathbf{G}_k \mathbf{H}$ is represented as

$$\mathbf{G}_k \mathbf{H} = \hat{\mathbf{C}}_k + \Delta \mathbf{C}_k, \quad k = 1, \dots, K, \quad (53)$$

where $\hat{\mathbf{C}}_k$ is the estimated cascaded CSI of BS-RIS-MU link at the k -th MU, and $\Delta \mathbf{C}_k$ is the unknown cascaded CSI given as

$$\|\Delta \mathbf{C}_k\|_F \leq \epsilon_k, \quad k = 1, \dots, K, \quad (54)$$

where ϵ_k is the radii of the uncertainty regions known at the BS, and we set $\epsilon_k = 0.5$ in simulation. The transmission rate maximization problem (52) is equivalent to

$$(P4) \quad \min_{\mathbf{v}, \mathbf{u}} \|\mathbf{v}\|^2 \quad (9), \quad (54), \quad (55)$$

$$\log \left(1 + \|(\mathbf{u}^H \mathbf{G}_k \mathbf{H} + \mathbf{t}_k^H) \mathbf{v}\|^2 \right) \geq R, \quad k = 1 \dots, K, \quad (56)$$

where R is the target transmission rate and constrains (56) are the worst-case SNR requirements for the MUs. From [38], we obtain that for the given optimal solution at the i -th $\{\mathbf{v}^{(i)}, \mathbf{u}^{(i)}\}$, $\|(\mathbf{u}^H \mathbf{G}_k \mathbf{H} + \mathbf{t}_k^H) \mathbf{v}\|^2$ is linearly approximated by its lower bound at $\{\mathbf{v}^{(i)}, \mathbf{u}^{(i)}\}$ as follows

$$\text{vec}^T(\Delta \mathbf{C}_k) \mathbf{A} \text{vec}(\Delta \mathbf{C}_k^*) + 2\text{Re}\{\mathbf{1}_k \text{vec}(\Delta \mathbf{C}_k^*)\} + \varphi_k, \quad (57)$$

where

$$\mathbf{A} = \mathbf{v} \mathbf{v}^{H,(i)} \otimes \mathbf{u} \mathbf{u}^{T,(i)} + \mathbf{v}^{(i)} \mathbf{v}^H \otimes \mathbf{u}^{(i)} \mathbf{u}^T - \mathbf{v}^{(i)} \mathbf{v}^{H,(i)} \otimes \mathbf{u}^{(i)} \mathbf{u}^{T,(i)}, \quad (58)$$

$$\begin{aligned} \mathbf{1}_k = & \text{vec} \left(\mathbf{u} \left(\mathbf{t}_k^H + \mathbf{u}^{H,(i)} \hat{\mathbf{C}}_k \right) \mathbf{v}^{(i)} \mathbf{v}^H \right) \\ & + \text{vec} \left(\mathbf{u}^{(i)} \left(\mathbf{t}_k^H + \mathbf{u}^H \hat{\mathbf{C}}_k \right) \mathbf{v} \mathbf{v}^{H,(i)} \right) \\ & - \text{vec} \left(\mathbf{u} \left(\mathbf{t}_k^H + \mathbf{u}^{H,(i)} \hat{\mathbf{C}}_k \right) \mathbf{v}^{(i)} \mathbf{v}^{H,(i)} \right), \end{aligned} \quad (59)$$

$$\begin{aligned} \varphi_k = & 2\text{Re} \left\{ \left(\mathbf{t}_k^H + \mathbf{u}^{H,(i)} \hat{\mathbf{C}}_k \right) \mathbf{v}^{(i)} \mathbf{v}^H \left(\mathbf{t}_k + \hat{\mathbf{C}}_k^H \mathbf{u} \right) \right\} \\ & - \left(\mathbf{t}_k^H + \mathbf{u}^{H,(i)} \hat{\mathbf{C}}_k \right) \mathbf{v}^{(i)} \mathbf{v}^{H,(i)} \left(\mathbf{t}_k + \hat{\mathbf{C}}_k^H \mathbf{u}^{(i)} \right). \end{aligned} \quad (60)$$

Thus, constraints (56) can be reformulated as

$$\text{vec}^T(\Delta \mathbf{C}_k) \mathbf{A} \text{vec}(\Delta \mathbf{C}_k^*) + 2\text{Re}\{\mathbf{1}_k \text{vec}(\Delta \mathbf{C}_k^*)\} + \varphi_k \geq 2^R - 1, \quad (61)$$

By general S-procedure [38], conditions (54) and (61) can be approximately rewritten as the linear matrix inequality, i.e.,

$$\begin{bmatrix} \varpi_k \mathbf{I} + \mathbf{A} & \mathbf{1}_k \\ \mathbf{1}_k^T & \varphi_k - (2^R - 1) - \varpi_k \epsilon_k \end{bmatrix} \succeq 0, \quad (62)$$

Based on (62), Problem (P4) can be approximately reformulated as

$$(P5) \quad \min_{\mathbf{v}, \mathbf{u}, \varpi} \|\mathbf{v}\|^2 \quad (9), \quad (62), \quad (63)$$

where $\varpi = [\varpi_1, \dots, \varpi_K]^T \geq 0$ are slack variables. Problem (P5) can be solved by the alternating optimization.

Optimization of \mathbf{v} with fixed \mathbf{u} : First, for the fixed \mathbf{u} , the subproblem is given as

$$(P5.1) \quad \min_{\mathbf{v}, \varpi} \|\mathbf{v}\|^2 \quad (9), (62), \quad (64)$$

which is convex problem and can be solved by SDP techniques.

Optimization of \mathbf{u} with fixed \mathbf{v} : Then, for the fixed \mathbf{v} , the subproblem of \mathbf{u} is a feasibility-check problem. By introducing slack variables β_k , $k = 1 \dots, K$, constraint (61) is modified as

$$\text{vec}^T(\Delta \mathbf{C}_k) \mathbf{A} \text{vec}(\Delta \mathbf{C}_k^*) + 2\text{Re}\{\mathbf{1}_k \text{vec}(\Delta \mathbf{C}_k^*)\} + \varphi_k \geq 2^R - 1 - \beta_k. \quad (65)$$

Thus, the constraint (62) can be modified as

$$\begin{bmatrix} \varpi_k \mathbf{I} + \mathbf{A} & \mathbf{1}_k \\ \mathbf{1}_k^T & \varphi_k - (2^R - 1) - \varpi_k \epsilon_k - \beta_k \end{bmatrix} \succeq 0, \quad (66)$$

and the subproblem for the fixed \mathbf{v} is formulated as

$$(P5.2) \quad \max_{\mathbf{v}, \varpi, \beta} \sum_{k=1}^K \beta_k \quad (9), (66), \quad (68)$$

$$\beta \geq \mathbf{0}, \quad (68)$$

where $\beta = [\beta_1, \dots, \beta_K]$. Problem (P5.2) is non-convex, and thus we adopt convex-concave procedure [39]. For the fixed $\Phi_n^{(j)}$, the non-convex part of the constraint (9) are linearized by $|\Phi_n^{(j)}|^2 - 2\text{Re}\{\Phi_n^* \Phi_n^{(j)}\} \leq -1$. Thus, Problem (P5.2) is solved by a sequence of problems, i.e.,

$$(P5.2^*) \quad \max_{\mathbf{v}, \varpi, \beta, \delta} \sum_{k=1}^K \beta_k - \iota^{(j)} \sum_{n=1}^N \delta_n \quad (9), (66) (68), \quad (69)$$

$$|\Phi_n^{(j)}|^2 - 2\text{Re}\{\Phi_n^* \Phi_n^{(j)}\} \leq \delta_n - 1, \quad (70)$$

$$|\Phi_n|^2 \leq 1 \quad n = 1 + \delta_n, \quad n = 1, \dots, N, \quad (71)$$

$$\delta \geq \mathbf{0}, \quad (72)$$

Here, $\delta = [\delta_1, \dots, \delta_M]$ are slack variables imposed over the equivalent linear constraints of constraint (9). $\sum_{n=1}^N \delta_n$ is the penalty term in the objective function (69). $\iota^{(j)}$ is a parameter to control the accuracy of the approximations. Obviously, when $\iota^{(j)}$ goes to infinity, Problems (P5.2*) and (P5.2) become same. It is notice that Problem (P5.2*) is convex, which can be solved by CVX. Based on above discussions, the alternating optimization for Problem(P4) is summarized as Algorithm 3.

Remark 5: It is worth to theoretically characterize the performance gap between the perfect CSI and the imperfect CSI. It is hard to the direct performance gap, since we cannot obtain the closed-form solution for the two cases. However, we can obtain the lower bound of the gap by comparing the lower bound of the prefect CSI case and the upper bound of the imperfect CSI case. To our best knowledge, there are no works considering to compute the upper bound of the imperfect CSI case, which will be an interesting research problem for future study.

Algorithm 3 Alternating Optimization for Problem (P4)

Input: \mathbf{G}_k , $k = 1, \dots, K$, \mathbf{H} , R , ι^0 , $\eta > 1$, and the error tolerances $\delta_1 > 0$ and $\delta_2 > 0$.

Output: $\{\mathbf{v}_*, \mathbf{u}_*\}$.

- 1: **Initialize** $\{\mathbf{v}^{(i)}, \mathbf{u}^{(i)}\}$ and $\mathbf{u}^{(j)}$, which represent the output of the i -th outer iteration and the input of the j -th inner iteration, respectively.
 - 2: **while** $\|\mathbf{v}^{(i)}\| - \|\mathbf{v}^{(i-1)}\| > \delta_1$ **do**
 - 3: Compute $\mathbf{v}^{(i+1)}$ by solving Problem (P5.1) with $\mathbf{u}^{(i)}$ and $\mathbf{v}^{(i)}$.
 - 4: **Initialize** $\iota^{(1)} = \iota^0$ and $\mathbf{u}^{(1)} = \mathbf{u}^{(i)}$.
 - 5: **while** $\|\mathbf{u}^{(j)} - \mathbf{u}^{(j-1)}\| > \delta_2$ **do**
 - 6: Compute $\mathbf{u}^{(j+1)}$ by solving Problem (P5.2*) with $\mathbf{u}^{(j)}$, $\mathbf{v}^{(i+1)}$, and $\iota^{(j)}$.
 - 7: $\iota^{(j+1)} = \eta \iota^{(j)}$.
 - 8: **end while**
 - 9: Let $\mathbf{u}^{(i+1)} = \mathbf{u}^{(j)}$.
 - 10: **end while**
 - 11: Let $\{\mathbf{v}_*, \mathbf{u}_*\} = \{\mathbf{v}^{(i+1)}, \mathbf{u}^{(i+1)}\}$.
-

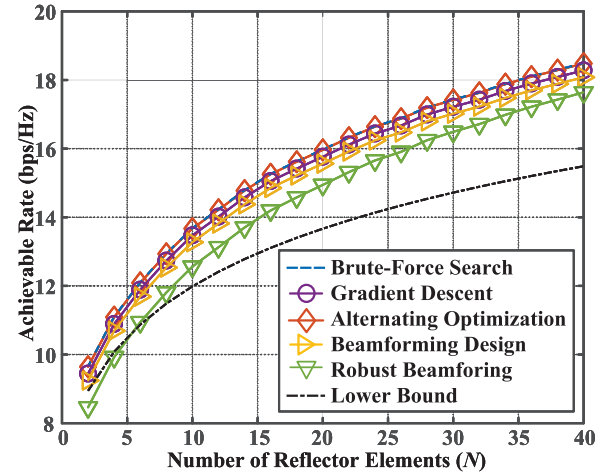


Fig. 3. Achievable rates versus the number of reflecting elements (N).

B. Performance Comparison

Fig. 3 shows the achievable rates versus the number of reflecting elements N , where $M = 8$, $K = 8$, $B = 1$, and $\rho = 20$ (dB). All the schemes with RIS are better than the scheme without RIS. The achievable rate for alternating optimization closes to the maximal capacity obtained by brute-force search, which proves that the alternating optimization has a brilliant performance. The proposed algorithms outperform the beamforming design scheme. This is because beamforming vector can be seen as one-rank covariance matrix \mathbf{Q} , and in most cases cannot achieves the capacity. The gaps between the curves of the proposed algorithms and the lower bound increase significantly. This is because with more reflecting elements, the RIS provides more degrees of freedom further to improve the BS-MU link with the worst channel condition and thus obtain the high gains.

Fig. 4 presents the achievable rates versus the Rician factor B , where $\rho = 20$ (dB), $N = 8$, and $M = 8$.

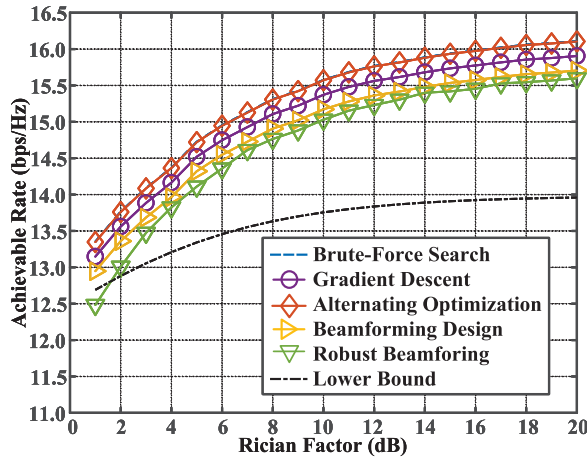
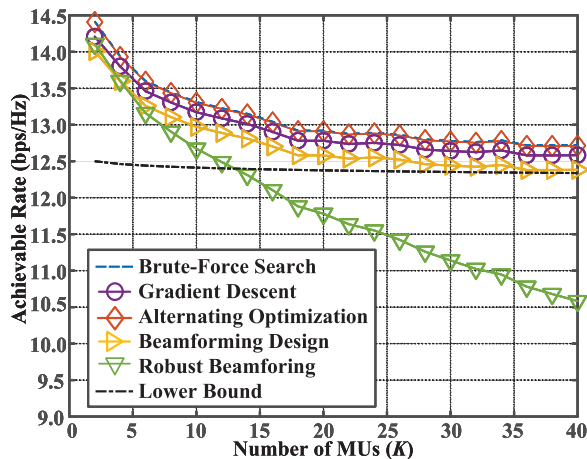
Fig. 4. Achievable rates versus the Rician factor (B).Fig. 5. Achievable rates versus the number of MUs (K).

Fig. 4 shows that the achievable rates first increase and then approach constants, which conforms Remark 4. It implies that only LoS components exist, and the channel coefficients remain unchanged. Please notice that the lower bound is the one of the capacity rather than the one of the achievable rate for the beamforming design. Thus, the lower bound is greater than achievable rate of the beamforming design when $B \leq 1.6$.

Fig. 5 shows the relationship between the achievable rates and the number of MUs K , where $N = 8$, $M = 8$, $B = 1$, and $\rho = 20$ (dB). From Fig. 5, we can observe that the achievable rates decrease with the increase in K . Notice that the gap of the curves between the robust beamforming and the capacity increase with K increasing. This is because the increase in K rises the uncertainty for robust beamforming design, which leads to the reduction of the achievable rate. The lower bound is given by (49), and the gap of the curves between the capacity and lower bound decrease.

Fig. 6 shows the achievable rates with identical K and M (i.e., $\frac{K}{M} = 1$), where $N = 8$ and $B = 1$. The lower bound given by (87) is a constant. The achievable rates rise firstly and then approach a finite value. It follows that the capacity is limited when M and K go to infinity at a ratio, which confirms Proposition 6.

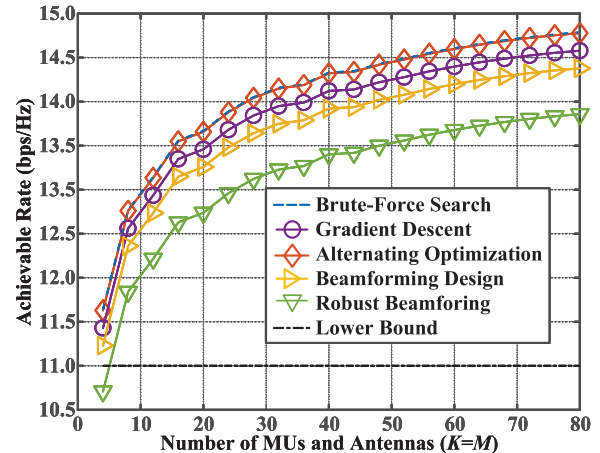
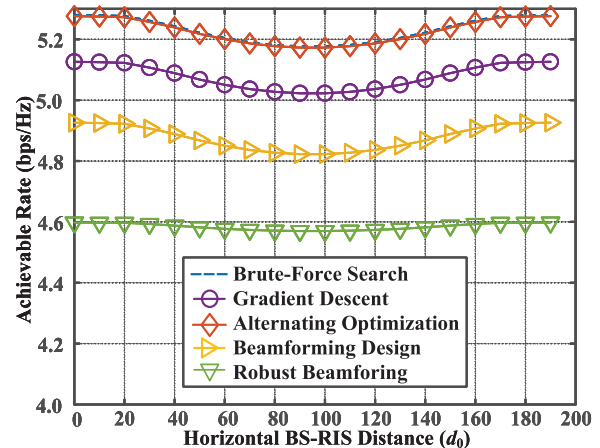
Fig. 6. Achievable rate versus the equal numbers of MUs (K) and antennas (M).Fig. 7. Achievable rate versus the equal numbers of MUs (K) and antennas (M).

Fig. 7 considers the effect of the path-loss in far-field communication. The 3GPP propagation environment described in [17]: 1) The large scale fading mode at distance d is given as $\frac{10^{-3.75}}{d^{3.75}}$; 2) The BS and RIS are located at $(0, 0)$ and $(d_0, 50m)$, respectively, where d_0 is the horizontal BS-RIS distance, and the MUs are randomly and uniformly placed in the circular region with centre $(150m, 0)$ and radius $50m$. Moreover, we set $K = 8$, $M = 8$, $N = 8$, $P_{\max} = 10$ dBW, and the power of noises is set as -80 dBm. From Fig. 7, it is concluded that the RIS near either the BS and MUs owns higher capacity than the RIS in the middle of BS and MUs. This is because the RIS near the BS can reflect a stronger signal from the BS, and the MU near the RIS is able to receive the stronger reflected signal from the RIS.

VI. CONCLUSION

This paper considered a RIS assisted multicast communication. First, we formulated a capacity optimization problem and proposed two algorithms to obtain the locally optimal covariance matrix and phase shifts. Then, this paper considered a special case, where we only need to optimize the MU with the worst channel condition. Lastly, we analyzed the order

growth for the optimal capacity of RIS assisted multicast transmission when the numbers of reflecting elements, BS antennas, and MUs go to infinity.

APPENDIX I PROOF OF PROPOSITION 4

It is obvious that C is smaller than the capacity of the channel from BS to any MUs, i.e.,

$$C \leq \max_{\theta} \log \left(1 + P_{\max} \|\mathbf{u}^H \mathbf{G}_k \mathbf{H} + \mathbf{t}_k^H\|^2 \right), \quad (73)$$

which is also an upper bound for C . From (3) and (2), we obtain

$$\mathbf{u}^H \mathbf{G}_k \mathbf{H} + \mathbf{t}_k^H = [\Psi_{1,k}, \Psi_{2,k}, \dots, \Psi_{m,k}], \quad (74)$$

where $\Psi_{m,k} = \sum_{n=1}^N g_{k,n,m} + t_{k,m}$, with $g_{k,n,m} = \Phi_n h_{k,n} H_{n,m}$. By the definitions in the first of section IV, we obtain $h_{k,n} \sim \mathcal{CN} \left(\sqrt{\frac{B}{B+1}} a_n, \frac{1}{B+1} \right)$, $H_{n,m} \sim \mathcal{CN} \left(\sqrt{\frac{B}{B+1}} a_n a_m, \frac{1}{B+1} \right)$, $t_{k,m} \sim \mathcal{CN} \left(\sqrt{\frac{B}{B+1}} a_m, \frac{1}{B+1} \right)$, where $a_n = e^{j2\pi \frac{\alpha}{\lambda} (n-1) \sin^2 \omega \cos \vartheta \sin \vartheta}$. Since $|\Phi_n| = 1$, $|a_n| = 1$ and $h_{k,n}$, $H_{n,m}$, $t_{k,m}$ are independent, it follows

$$\begin{aligned} \mathbb{E} \left\{ |\Psi_{m,k}|^2 \right\} &= \left(N \frac{B}{B+1} + \sqrt{\frac{B}{B+1}} \right)^2 \\ &+ N \left(\left(\frac{B}{B+1} + \frac{1}{B+1} \right)^2 - \left(\frac{B}{B+1} \right)^2 \right) \\ &+ \frac{1}{B+1} = A(N^2). \end{aligned} \quad (75)$$

Then, based on the law of large numbers and (75), it follows

$$\|\mathbf{u}^H \mathbf{G}_k \mathbf{H} + \mathbf{t}_k^H\|^2 = \sum_{m=1}^M |\Psi_{m,k}|^2 \quad (76)$$

$$\begin{aligned} &\rightarrow M \mathbb{E} \left\{ |\Psi_{m,k}|^2 \right\} \\ &= MA(N^2), \end{aligned} \quad (77)$$

a.s., as $M \rightarrow \infty$. Thus, C is upper bounded by

$$\log \left(1 + P_{\max} MA(N^2) \right). \quad (78)$$

Next, from [32], it is obtained that C is lower bounded in

$$\max_{\theta} \log \left(1 + \frac{P_{\max}}{K^2} \|\mathbf{u}^H \mathbf{G}_k \mathbf{H} + \mathbf{t}_k^H\|^2 \right). \quad (79)$$

By the same proof for the upper bound of C , the lower bound of that can be rewritten as

$$\begin{aligned} &\max_{\theta} \log \left(1 + \frac{P_{\max}}{K^2} \|\mathbf{u}^H \mathbf{G}_k \mathbf{H} + \mathbf{t}_k^H\|^2 \right) \\ &\rightarrow \log \left(1 + P_{\max} \frac{MA(N^2)}{K^2} \right), \end{aligned} \quad (80)$$

a.s., as $M \rightarrow \infty$.

From the upper and lower bounds in (78) and (80), we obtain that

- When K and N are fixed and M goes to infinity, both the upper and lower bounds of C are $\mathcal{O}(\log M)$, and it follows (40);

- When N and M go to infinity and K is fixed, both the upper and lower bounds of C are $\mathcal{O}(\log N^2 M)$, and it follows (42).

Last, the proof of (41) is similar to that of (40) and (42), and thus we only show its difference. By the law of large number, we can obtain that as $N \rightarrow \infty$,

$$\begin{aligned} |\Psi_{m,k}|^2 &= \left(\sum_{i=1}^N g_{k,n,m} + t_{k,m} \right) \left(\sum_{n=1}^N \bar{g}_{k,i,m} + \bar{t}_{k,m} \right) \\ &\rightarrow \sum_{n=1}^N \sum_{i=1, i \neq n}^N \mathbb{E} \{ g_{k,n,m} \bar{g}_{k,i,m} \} + \sum_{n=1}^N \mathbb{E} \left\{ |g_{k,n,m}|^2 \right\} \\ &\quad + 2 \sum_{n=1}^N \mathbb{E} \{ g_{k,n,m} \bar{t}_{k,m} \} + \mathbb{E} \left\{ |t_{k,m}|^2 \right\} \quad (81) \\ &= \left(N \frac{B}{B+1} + \sqrt{\frac{B}{B+1}} \right)^2 \\ &\quad + N \left(1 - \left(\frac{B}{B+1} \right)^2 \right) + \frac{1}{B+1} = A(N^2), \end{aligned} \quad (82)$$

It follows $\|\mathbf{u}^H \mathbf{G}_k \mathbf{H} + \mathbf{t}_k^H\|^2 = MA(N^2)$, as $N \rightarrow \infty$. The other steps of this proof is same to the proof of (40) and (42), and thus is omitted.

APPENDIX II PROOF OF PROPOSITION 6

We first show the lower bound of $\mathbb{E}\{C\}$. From the proof of Propositions 4, we obtain that the mean of $\|\mathbf{u}^H \mathbf{G}_k \mathbf{H} + \mathbf{t}_k^H\|^2$ is $MA(N^2)$ and the variance of that is $MD(N^3)$, where

$$\begin{aligned} D(N^3) &= 4 \left(\left(1 - \left(\frac{B}{B+1} \right)^2 \right) N + \frac{1}{B+1} \right) \\ &\quad \left(\frac{NB}{B+1} + \sqrt{\frac{B}{B+1}} \right)^2 \\ &\quad + 2 \left(\left(1 - \left(\frac{B}{B+1} \right)^2 \right) N + \frac{1}{B+1} \right)^2. \end{aligned} \quad (83)$$

It follows that the mean and variance of $\frac{\|\mathbf{u}^H \mathbf{G}_k \mathbf{H}\|^2}{M}$ are $A(N^2)$ and $\frac{D(N^3)}{M}$, respectively. Therefore, letting $l \leq \frac{1}{B+1} (N+2)/2 + \frac{B}{B+1} (N+1)^2$, we derive

$$\begin{aligned} &P \left\{ \frac{\|\mathbf{u}^H \mathbf{G}_k \mathbf{H} + \mathbf{t}_k^H\|^2}{M} \leq l \right\} \\ &= P \left\{ \frac{\|\mathbf{u}^H \mathbf{G}_k \mathbf{H} + \mathbf{t}_k^H\|^2}{M} - A(N^2) \leq (l - A(N^2)) \right\} \\ &\leq P \left\{ \left| \frac{\|\mathbf{u}^H \mathbf{G}_k \mathbf{H} + \mathbf{t}_k^H\|^2}{M} - A(N^2) \right| \geq (A(N^2) - l) \right\} \\ &\leq \frac{D(N^3)}{M(A(N^2) - l)^2}, \end{aligned} \quad (84)$$

where (84) is due to Chebyshev inequality. By the extreme value theory [40], we obtain

$$P \left\{ \min_{k=1, \dots, K} \frac{\|\mathbf{u}^H \mathbf{G}_k \mathbf{H} + \mathbf{t}_k^H\|^2}{M} \geq l \right\} = \left(1 - P \left\{ \frac{\|\mathbf{u}^H \mathbf{G}_k \mathbf{H} + \mathbf{t}_k^H\|^2}{M} \leq l \right\} \right)^K. \quad (85)$$

Then, combing (84) and (85), it is obtained that

$$P \left\{ \min_{k=1, \dots, K} \frac{\|\mathbf{u}^H \mathbf{G}_k \mathbf{H} + \mathbf{t}_k^H\|^2}{M} \geq l \right\} = \left(1 - \frac{D(N^3)}{M(A(N^2) - l)^2} \right)^K \rightarrow \exp \left(-\frac{KD(N^3)}{M(A(N^2) - l)^2} \right), \quad (86)$$

as $K \rightarrow \infty$. It is obvious that the lower bound of $\mathbb{E}\{C\}$ is given as

$$\begin{aligned} \mathbb{E}\{C\} &\geq \mathbb{E} \log \left(1 + P_{\max} \min_{k=1, \dots, K} \frac{\|\mathbf{u}^H \mathbf{G}_k \mathbf{H} + \mathbf{t}_k^H\|^2}{M} \right) \\ &\geq P \left\{ \min_{k=1, \dots, K} \frac{\|\mathbf{u}^H \mathbf{G}_k \mathbf{H} + \mathbf{t}_k^H\|^2}{M} \geq l \right\} \\ &\quad \log(1 + lP_{\max}) \\ &\rightarrow \exp \left(-\frac{KD(N^3)}{M(A(N^2) - l)^2} \right) \log(1 + lP_{\max}), \quad (87) \end{aligned}$$

as $K \rightarrow \infty$, where (87) is due to (86). From (87), it is easy to see that since $l < A(N^2)$ and $\frac{K}{M} \leq \infty$ is a fixed ratio, the lower bounds of $\mathbb{E}\{C\}$ are both $\mathcal{O}(1)$ for the case of fixed N and $N \rightarrow \infty$ cases, respectively.

Next, we show the upper bound of $\mathbb{E}\{C\}$. For the minimum received SNR, we derive

$$\begin{aligned} \max_{\mathbf{Q}} \min_{k=1, \dots, K} (\mathbf{u}^H \mathbf{G}_k \mathbf{H} + \mathbf{t}_k^H) \mathbf{Q} (\mathbf{H}^H \mathbf{G}_k^H \mathbf{u} + \mathbf{t}_k) \\ \leq \frac{1}{K} \max_{\mathbf{Q}} \sum_{k=1}^K (\mathbf{u}^H \mathbf{G}_k \mathbf{H} + \mathbf{t}_k^H) \mathbf{Q} (\mathbf{H}^H \mathbf{G}_k^H \mathbf{u} + \mathbf{t}_k) \quad (88) \\ = \frac{1}{K} \max_{\mathbf{Q}} \text{Tr}(\mathbf{Q} \mathbf{\Omega} \mathbf{\Omega}^H) \quad (89) \\ = \frac{P_{\max}}{K} \lambda_{\max}(\mathbf{\Omega} \mathbf{\Omega}^H), \quad (90) \end{aligned}$$

where $\mathbf{\Omega} = [\mathbf{H}^H \mathbf{G}_1^H \mathbf{u} + \mathbf{t}_1, \dots, \mathbf{H}^H \mathbf{G}_K^H \mathbf{u} + \mathbf{t}_K]$; (88) is due to the fact that the minimum received SNR is upper bounded by the average received SNR; (90) is due to the fact that the maximization (89) is equivalent to the maximal eigenvalue of the matrix $\lambda_{\max}(\mathbf{\Omega} \mathbf{\Omega}^H)$ [34]. From the eigenvalue of random matrix theory [41] ($\Psi_{m,k}$ is elements of matrix $\mathbf{\Omega}$), we obtain

$$\frac{P_{\max}}{K} \lambda_{\max}(\mathbf{\Omega} \mathbf{\Omega}^H) \rightarrow P_{\max} A(N^2) \left(1 + \sqrt{\frac{M}{K}} \right)^2, \quad (91)$$

a.s., as $K \rightarrow \infty$, $M \rightarrow \infty$ and $\frac{K}{M} < \infty$, which implies

$$C \leq \log \left(1 + P_{\max} A(N^2) \left(1 + \sqrt{\frac{M}{K}} \right)^2 \right). \quad (92)$$

It follows $\mathbb{E}\{C\} \leq \mathcal{O}(1)$ for the fixed N , and $\mathbb{E}\{C\} \leq \mathcal{O}(\log(N^2))$ for the $N \rightarrow \infty$.

REFERENCES

- [1] Cisco Visual Networking Index: Global Mobile Data Traffic Forecast Update, 2017-2022 White Paper, Cisco, San Jose, CA, USA, Feb. 2019.
- [2] B. Zhou, Y. Cui, and M. Tao, "Optimal dynamic multicast scheduling for cache-enabled content-centric wireless networks," *IEEE Trans. Commun.*, vol. 65, no. 7, pp. 2956–2970, Jul. 2017.
- [3] M. R. A. Khandaker and Y. Rong, "Precoding design for MIMO relay multicasting," *IEEE Trans. Wireless Commun.*, vol. 12, no. 7, pp. 3544–3555, Jul. 2013.
- [4] W. Saad, M. Bennis, and M. Chen, "A vision of 6G wireless systems: Applications, trends, technologies, and open research problems," *IEEE Netw.*, vol. 34, no. 3, pp. 134–142, May 2020.
- [5] M. D. Renzo *et al.*, "Smart radio environments empowered by reconfigurable AI meta-surfaces: An idea whose time has come," *EURASIP J. Wireless Commun. Netw.*, vol. 2019, no. 1, pp. 1–20, Dec. 2019.
- [6] C. Liaskos, S. Nie, A. Tsioliaridou, A. Pitsillides, S. Ioannidis, and I. Akyildiz, "A new wireless communication paradigm through software-controlled metasurfaces," *IEEE Commun. Mag.*, vol. 56, no. 9, pp. 162–169, Sep. 2018.
- [7] G. Yang, X. Xu, Y.-C. Liang, and M. D. Renzo, "Reconfigurable intelligent surface-assisted non-orthogonal multiple access," *IEEE Trans. Wireless Commun.*, vol. 20, no. 5, pp. 3137–3151, May 2021.
- [8] C. Huang, R. Mo, and C. Yuen, "Reconfigurable intelligent surface assisted multiuser MISO systems exploiting deep reinforcement learning," *IEEE J. Sel. Areas Commun.*, vol. 38, no. 8, pp. 1839–1850, Aug. 2020.
- [9] G. Yang, Y.-C. Liang, R. Zhang, and Y. Pei, "Modulation in the air: Backscatter communication over ambient OFDM carrier," *IEEE Trans. Commun.*, vol. 66, no. 3, pp. 1219–1233, Mar. 2018.
- [10] G. Yang, Q. Zhang, and Y.-C. Liang, "Cooperative ambient backscatter communications for green Internet-of-Things," *IEEE Internet Things J.*, vol. 5, no. 2, pp. 1116–1130, Apr. 2018.
- [11] Q. Wu and R. Zhang, "Towards smart and reconfigurable environment: Intelligent reflecting surface aided wireless network," *IEEE Commun. Mag.*, vol. 58, no. 1, pp. 106–112, Jan. 2020.
- [12] M. Di Renzo *et al.*, "Reconfigurable intelligent surfaces vs. relaying: Differences, similarities, and performance comparison," *IEEE Open J. Commun. Soc.*, vol. 1, pp. 798–807, Jun. 2020.
- [13] S. Hu, F. Rusek, and O. Edfors, "Beyond massive MIMO: The potential of data transmission with large intelligent surfaces," *IEEE Trans. Signal Process.*, vol. 66, no. 10, pp. 2746–2758, May 2018.
- [14] E. Bjornson, O. Ozdogan, and E. G. Larsson, "Intelligent reflecting surface versus decode-and-forward: How large surfaces are needed to beat relaying?" *IEEE Wireless Commun. Lett.*, vol. 9, no. 2, pp. 244–248, Feb. 2020.
- [15] Y. Han, W. Tang, S. Jin, C.-K. Wen, and X. Ma, "Large intelligent surface-assisted wireless communication exploiting statistical CSI," *IEEE Trans. Veh. Technol.*, vol. 68, no. 8, pp. 8238–8242, Aug. 2019.
- [16] S. Li, B. Duo, X. Yuan, Y.-C. Liang, and M. Di Renzo, "Reconfigurable intelligent surface assisted UAV communication: Joint trajectory design and passive beamforming," *IEEE Wireless Commun. Lett.*, vol. 9, no. 5, pp. 716–720, May 2020.
- [17] C. Huang, A. Zappone, G. C. Alexandropoulos, M. Debbah, and C. Yuen, "Reconfigurable intelligent surfaces for energy efficiency in wireless communication," *IEEE Trans. Wireless Commun.*, vol. 18, no. 8, pp. 4157–4170, Aug. 2019.
- [18] M. Cui, G. Zhang, and R. Zhang, "Secure wireless communication via intelligent reflecting surface," *IEEE Wireless Commun. Lett.*, vol. 8, no. 5, pp. 1410–1414, Oct. 2019.
- [19] Z. Chu, W. Hao, P. Xiao, and J. Shi, "Intelligent reflecting surface aided multi-antenna secure transmission," *IEEE Wireless Commun. Lett.*, vol. 9, no. 1, pp. 108–112, Jan. 2020.
- [20] L. You, J. Wang, W. Wang, and X. Gao, "Secure multicast transmission for massive MIMO with statistical channel state information," *IEEE Signal Process. Lett.*, vol. 26, no. 6, pp. 803–807, Jun. 2019.

- [21] L. Du, C. Huang, W. Guo, J. Ma, X. Ma, and Y. Tang, "Reconfigurable intelligent surfaces assisted secure multicast communications," *IEEE Wireless Commun. Lett.*, vol. 9, no. 10, pp. 1673–1676, Oct. 2020.
- [22] G. Zhou, C. Pan, H. Ren, K. Wang, and A. Nallanathan, "A framework of robust transmission design for IRS-aided MISO communications with imperfect cascaded channels," *IEEE Trans. Signal Process.*, vol. 68, pp. 5092–5106, Aug. 2020.
- [23] L. Wei, C. Huang, G. C. Alexandropoulos, C. Yuen, Z. Zhang, and M. Debbah, "Channel estimation for RIS-empowered multi-user MISO wireless communications," *IEEE Trans. Commun.*, early access, Mar. 2, 2021, doi: [10.1109/TCOMM.2021.3063236](https://doi.org/10.1109/TCOMM.2021.3063236).
- [24] S. Zhang and R. Zhang, "Capacity characterization for intelligent reflecting surface aided MIMO communication," *IEEE J. Sel. Areas Commun.*, vol. 38, no. 8, pp. 1823–1838, Aug. 2020.
- [25] J. Zhang, C. Qi, P. Li, and P. Lu, "Channel estimation for reconfigurable intelligent surface aided massive MIMO system," in *Proc. IEEE 21st Int. Workshop Signal Process. Adv. Wireless Commun. (SPAWC)*, May 2020, pp. 1–5.
- [26] Z. Wang, L. Liu, and S. Cui, "Channel estimation for intelligent reflecting surface assisted multiuser communications: Framework, algorithms, and analysis," *IEEE Trans. Wireless Commun.*, vol. 19, no. 10, pp. 6607–6620, Oct. 2020.
- [27] B. Zheng and R. Zhang, "Intelligent reflecting surface-enhanced OFDM: Channel estimation and reflection optimization," *IEEE Wireless Commun. Lett.*, vol. 9, no. 4, pp. 518–522, Apr. 2020.
- [28] B. Zheng, C. You, and R. Zhang, "Fast channel estimation for IRS-assisted OFDM," *IEEE Wireless Commun. Lett.*, vol. 10, no. 3, pp. 580–584, Mar. 2021.
- [29] B. Zheng, C. You, and R. Zhang, "Intelligent reflecting surface assisted multi-user OFDMA: Channel estimation and training design," *IEEE Trans. Wireless Commun.*, vol. 19, no. 12, pp. 8315–8329, Dec. 2020.
- [30] J. Zhao, "Optimizations with intelligent reflecting surfaces (IRSs) in 6G wireless networks: Power control, quality of service, max-min fair beamforming for unicast, broadcast, and multicast with multi-antenna mobile users and multiple IRSs," Aug. 2019, *arXiv:1908.03965*. [Online]. Available: <http://arxiv.org/abs/1908.03965>
- [31] G. Zhou, C. Pan, H. Ren, K. Wang, and A. Nallanathan, "Intelligent reflecting surface aided multigroup multicast miso communication systems," *IEEE Trans. Signal Process.*, vol. 68, pp. 3236–3251, 2020.
- [32] N. Jindal and Z.-Q. Luo, "Capacity limits of multiple antenna multicast," in *Proc. IEEE Int. Symp. Inf. Theory*, Jul. 2006, pp. 1841–1845.
- [33] S. Y. Park and D. J. Love, "Capacity limits of multiple antenna multicasting using antenna subset selection," *IEEE Trans. Signal Process.*, vol. 56, no. 6, pp. 2524–2534, Jun. 2008.
- [34] S. Boyd and L. Vandenberghe, *Convex Optimization*. Cambridge, UK: Cambridge Univ. Press, 2004.
- [35] A. S. Nemirovski and M. J. Todd, "Interior-point methods for optimization," *Acta Numer.*, vol. 17, pp. 191–234, May 2008.
- [36] M. Grant and S. Boyd. (Mar. 2014). *CVX: MATLAB Software for Disciplined Convex Programming, Version 2.1*. [Online]. Available: <http://cvxr.com/cvx>
- [37] J. M. Ortega and W. C. Rheinboldt, *Iterative Solution of Nonlinear Equations in Several Variables*. Philadelphia, PA, USA: SIAM, 1970.
- [38] S. Boyd, L. El Ghaoui, E. Feron, and V. Balakrishnan, *Linear Matrix Inequalities in System and Control Theory* (Studies in Applied Mathematics), vol. 15. Philadelphia, PA, USA: SIAM, Jun. 1994.
- [39] T. Lipp and S. Boyd, "Variations and extension of the convex-concave procedure," *Optim. Eng.*, vol. 17, no. 2, pp. 263–287, Jun. 2016.
- [40] M. Fisz and R. Bartoszyński, *Probability Theory and Mathematical Statistics*. New York, NY, USA: Wiley, 2018.
- [41] Z. D. Bai and Y. Q. Yin, "Limit of the smallest eigenvalue of a large dimensional sample covariance matrix," *Ann. Probab.*, vol. 21, no. 3, pp. 1275–1294, Jul. 1993.



Linsong Du (Student Member, IEEE) received the B.S. degree in electrical engineering from Sichuan Normal University, Chengdu, China, in 2015, and the M.S. degree from the University of Electronic Science and Technology of China, Chengdu, where he is currently pursuing the Ph.D. degree. His current research interests include energy harvesting communications, full-duplex communications, RIS assisted communications, information theory, and digital pre-distortion. He had been a TPC Member of GLOBECOM 2019. He is also a Reviewer of the IEEE WIRELESS COMMUNICATION LETTERS and IEEE ACCESS.



Shihai Shao (Member, IEEE) was born in Liaoning, China, in 1980. He received the B.E. and Ph.D. degrees in communication and information systems from the University of Electronic Science and Technology of China, Chengdu, China, in 2003 and 2008, respectively. Since 2008, he has been with the National Key Laboratory of Science and Technology on Communications, University of Electronic Science and Technology of China, as a Professor. His research interests include full-duplex communications, signal processing in wireless communications, spread spectra, and MIMO detection.



Gang Yang (Member, IEEE) received the B.Eng. and M.Eng. degrees (Hons.) in communication engineering, communication, and information systems from the University of Electronic Science and Technology of China, Chengdu, China, in 2008 and 2011, respectively, and the Ph.D. degree from Nanyang Technological University, Singapore, in 2015.

He was a Post-Doctoral Researcher with the Department of Electrical and Computer Engineering, National University of Singapore, in 2015. He is currently an Associate Professor with the National Key Laboratory of Science and Technology on Communications, and the Center for Intelligent Networking and Communications (CINC), University of Electronic Science and Technology of China. His current research interests include reconfigurable-reflecting-surface empowered communications, symbiotic radio based on backscatter communications, the Internet-of-Things communications, and wireless powered communications. He was a recipient of the IEEE Communications Society Stephen O. Rice Prize Paper Award in 2021, the IEEE Communications Society Transmission, Access, and Optical Systems (TAOS) Technical Committee Best Paper Award in 2016, and the Chinese Government Award for Outstanding Self-Financed Students Abroad in 2015. He served as the Publicity Co-Chair for the IEEE GLOBECOM 2017. He is also an Associate Editor of IEEE OPEN JOURNAL OF THE COMMUNICATIONS SOCIETY.



Jianhui Ma (Member, IEEE) received the M.S. degree from the University of Electronic Science and Technology of China, Chengdu, China, where he is currently pursuing the Ph.D. degree. His current research interests include relay communications, full-duplex communications, and anti-jamming communications. He had been a TPC Member of GLOBECOM 2019. He is also a Reviewer of the IEEE WIRELESS COMMUNICATIONS LETTERS.



Qingpeng Liang (Member, IEEE) received the B.E. degree in applied mathematics from the University of Electronic Science and Technology of China, Chengdu, China, in 2013, and the Ph.D. degree in control science and engineering from the School of Automation Engineering, University of Electronic Science and Technology of China, in 2020. He is currently an Assistant Professor with Southwest Jiaotong University, Chengdu. His research interests include full-duplex communications, information theory, and distributed control of multi-agent systems.



Youxi Tang (Member, IEEE) was born in Henan, China, in 1964. He received the B.E. degree in radar engineering from the College of PLA Ordnance, Shijiazhuang, China, in 1985, and the M.S. and Ph.D. degrees in communications and information systems from UESTC, Chengdu, China, in 1993 and 1997, respectively. From 1998 to 2000, he was with Huawei Technologies Company Ltd., Shanghai, China, as the Program Manager, working in the area of IS95 mobile communications and third-generation mobile communications. Since 2000, he has been with the National Key Laboratory of Science and Technology on Communications, UESTC, as a Professor. His general research interests include spread spectrum systems and wireless mobile systems, with the emphasis on signal processing in communications.